Electronic Supplementary Information

Continuous-Flow Synthesis of Organic Urea Derivatives from CO_2-Absorbed Alkanolamines over CeO_2 Catalyst

Shogen Mihara,[a,†] Natsuki Mizutani,[a,†] Hikari Terada,[a,†] Mizuho Yabushita,[a] Takaaki Endo,[b]

Yoshinao Nakagawa,[a] Akira Nakayama,[b] Keiichi Tomishige[a,c,*]

[a]Department of Applied Chemistry, Graduate School of Engineering, Tohoku University, 6-6-07 Aoba, Aramaki, Aoba-ku, Sendai, Miyagi 980-8579, Japan
[b]Department of Chemical System Engineering, Graduate School of Engineering, The University of Tokyo, Tokyo 113-8656, Japan
[c]Advanced Institute for Materials Research (WPI-AIMR), Tohoku University, 2-1-1 Katahira, Aoba-ku, Sendai, Miyagi 980-8577, Japan

*Corresponding author: tomishige@tohoku.ac.jp
[†]These authors contributed equally to this work.

[**Calculation of the amount of CO_2 released from (2-hydroxyethyl)carbamic salt (2AOL-CA)**]

The amount of CO_2 released from 2AOL-CA via its thermal decomposition in 2-propanol solvent within the batch reactor (inner volume 190 mL) was calculated based on the data in Fig. 3A as follows. In this calculation, the released CO_2 was assumed to behave as an ideal gas. The reported density of 2-propanol (681 kg m^{-3} at 393 K under 1.5 MPa)[S1] was used to determine the dead volume of the autoclave.

$PV = nRT$ (S1)

The parameters were defined as:

$P = 0.1$ [MPa] $= 0.1 \times 10^6$ [Pa]

$$V = 190 \text{ [mL]} - \frac{0.200 \text{ [mol]} \times 60.1 \text{ [g mol}^{-1}\text{]}}{0.681 \text{ [g mL}^{-1}\text{]}} = 172 \text{ [mL]} = 0.172 \text{ [L]}$$

$T = 393$ [K]

$R = 8.3 \times 10^3$ [Pa L K^{-1} mol^{-1}]

Substituting these values into eq. S1, the moles of CO_2 released were calculated as:

$$n = \frac{PV}{RT} = \frac{0.1 \times 10^6 \times 0.172}{8.3 \times 10^3 \times 393} = 5 \times 10^{-3} \text{ [mol]} = 5 \text{ [mmol]} \quad \text{(S2)}$$

Thus, *ca.* 5 mmol of CO_2 was released from 2AOL-CA via its thermal decomposition under the described conditions.

[**Kinetic fitting analysis for the conversion of 2AOL-CA and 3AOL-CA**]

To compare the rates of the cyclization and ring-opening steps, we analyzed the dependence of the conversion of 2AOL-CA and 3AOL-CA on $W_{cat}/F_{substrate}$ at 393 K (Figs. 4 and 6) by kinetic fitting. For tractability, all elementary steps were treated as pseudo-first-order with respect to the substrate concentration, and reverse reactions were not taken into account, as represented below:

$$n\text{AOL-CA} \xrightarrow{k_1} n\text{CC} \xrightarrow{k_2} n\text{LU} \quad \text{(S3)}$$

Here, k_1 and k_2 (unit: mmol g^{-1} h^{-1}) are the first-order rate constants for each reaction step. Because the solvent (*n*AOL) is present in large excess relative to *n*AOL-CA and *n*CC, its concentration was considered as constant. In this analysis, the contact time t, which is the same as $W_{cat}/F_{substrate}$ (unit = g h $mmol^{-1}$), was used for the calculations; accordingly, k_1 and k_2 have units of mmol g^{-1} h^{-1}. Under these assumptions, the differential kinetic equations for each compound as functions of t are:

$$\frac{\mathrm{d}[n\text{AOL-CA}]}{\mathrm{d}t} = -k_1[n\text{AOL-CA}] \quad \text{(S4)}$$

$$\frac{\mathrm{d}[n\text{CC}]}{\mathrm{d}t} = k_1[n\text{AOL-CA}] - k_2[n\text{CC}] \quad \text{(S5)}$$

$$\frac{\mathrm{d}[n\text{LU}]}{\mathrm{d}t} = k_2[n\text{CC}] \quad \text{(S6)}$$

In these equations, [*n*AOL-CA], [*n*CC], and [*n*LU] (unit: M) represent the concentrations of *n*AOL-CA, *n*CC, and *n*LU, respectively. These equations were integrated into the following equations:

$$[n\text{AOL-CA}] = [n\text{AOL-CA}]_{t=0}e^{-k_1 t} \quad \text{(S7)}$$

$$[n\text{CC}] = \frac{k_1}{k_2-k_1}[n\text{AOL-CA}]_{t=0}\left(e^{-k_1 t} - e^{-k_2 t}\right) \quad \text{(S8)}$$

$$[n\text{LU}] = [n\text{AOL-CA}]_{t=0}\left(1 - \frac{k_2 e^{-k_1 t} - k_1 e^{-k_2 t}}{k_2-k_1}\right) \quad \text{(S9)}$$

The contact time at which [*n*CC] reaches its maximum (*i.e.*, t_{max}) is:

$$t_{max} = \frac{1}{k_2-k_1}\ln\frac{k_1}{k_2} \quad \text{(S10)}$$

The experimental data at 393 K in kinetic region were fitted with these equations, and the results are shown in Fig. S10 and Table S11. In both reactions, the second step—the ring-opening reaction of *n*CC by *n*AOL to give *n*LU; n = 2 and 3)—proceeded faster than the cyclization of *n*AOL-CA to *n*CC, demonstrating the first step (*i.e.*, the cyclization of *n*AOL-CA) as the rate-determining step. Moreover, k_1 for the cyclization of 2AOL-CA exceeded that for 3AOL-CA, consistent with the thermodynamic favorability of the formation of five-membered-ring over that of six-membered ring.[S2,S3]

[**Identification and quantification of 4-aminobutyl *N*-(4-hydroxybutyl)carbamate (4LC)**]

To identify the products formed from the conversion of (4-hydroxybutyl)carbamic salt (4AOL-CA) in 4-amino-1-butanol (4AOL) solvent, we prepared 4AOL-CA from 4AOL and ^{13}C-labeled CO_2 in the same manner described in Section 2.2. The use of ^{13}C-labeled CO_2 was intended to enhance the NMR signals corresponding to carbonyl carbons in the 4AOL-CA-derived products.

The prepared ^{13}C-labeled 4AOL-CA in 4AOL was subjected to catalytic conversion in the fixed-bed flow reactor. Figs. S17A and S17B display the ^{13}C NMR spectrum of the reaction mixture after the conversion of ^{13}C-labeled 4AOL-CA. In the range of chemical shift between *ca.* 160–170 ppm, four distinct peaks were observed at 159.6 ppm, 161.3 ppm, 165.4 ppm, and 168.6 ppm. Among these, the peak at 165.4 ppm was attributed to the carbonyl carbon of the carbamate moiety in 4AOL-CA. The peak at 168.6 ppm was assignable to the carbon atom in the carbonate species (CO_3^{2-}) since the dissolution of amine and CO_2 into D_2O was known to generate such bicarbonate species.[S4] The absence of any cross peak for this ^{13}C signal in the ^{1}H–^{13}C HMBC spectrum (Fig. S18) further evidenced the lack of nearby protons within two to four bonds, supporting this assignment. Comparison with the reference ^{13}C NMR spectra of methyl *N*-butyl carbamate, *N*,*N*'-dibutylurea, and dibutyl carbonate (Fig. S19) revealed that the carbonyl carbons of carbonate, carbamate, and urea moieties appear at slightly different chemical shifts. Based on this comparsion, the peaks at 161.3 ppm and 159.6 ppm in Fig. S17 were assigned to the carbonyl carbons in 4LU and 4LC, respectively. The combination of ^{13}C NMR (Fig. S17A and S17B) and ^{1}H–^{13}C HMBC (Fig. S18) enabled the identification of the proton signals adjacent to the carbonate moiety in 4LC in the corresponding ^{1}H NMR spectra (Figs. S17C and S17D). Furthermore, 4LC was isolated successfully from the reaction mixture using an HPLC equipped with a fraction collector. The ^{1}H NMR spectrum of the isolated 4LC is shown in Fig. S20, which confirmed the assignment described above. Therefore, the quantification of 4LC involved in reaction mixtures was achieved by ^{1}H NMR spectroscopy in the presence of *tert*-butyl alcohol as an internal standard.

Table S1. Previous reports of direct conversions of alkylcarbamic salts into organic urea derivatives and organic carbamates.[a]

Entry	Alkylcarbamic salt (amount or feed rate)	Catalyst (mmol)	Additive (mmol)	Solvent (mL)	Atm. (MPa)	Temp. /K	Time /h	Reactor type	Target product(s) (yield /%)	Conv. /%	Sel. /%	Ref.
1	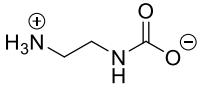 (10 mmol)	$Cp_2Ti(OTf)_2$ (0.04)	–	DMI (4.5)	n.r.	443	24	Batch	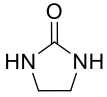 (99)	n.r.	n.r.	S5
2	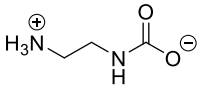 (19.6 mmol)	CeO_2 (2.0)	–	2-Propanol (15)	Ar (1)	413	24	Batch	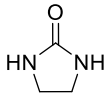 (83)	83	>99	S6
3	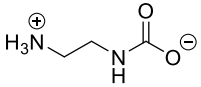 (5 mmol)	NR-CeO_2 (0.100)	–	2-Propanol (8)	Ar (3)	413	30	Batch	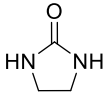 (92)	n.r.	n.r.	S7
4	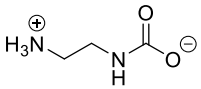 (20 mmol)	CeO_2 (2.0)	–	EDA (6.7)	Ar (1)	413	16	Batch	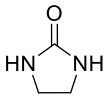 (62) 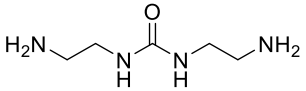 (38)	100	62 (upper product) 38 (lower product)	S8
5	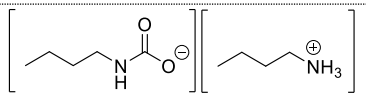 (10 mmol)	CeO_2 (2.0)	–	Butylamine (9.9)	Ar (1)	433	72	Batch	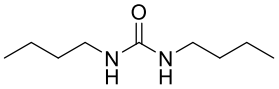 (74)	n.r.	n.r.	S8
6	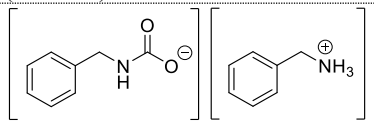 (10 mmol)	CeO_2 (2.0)	–	Benzylamine (11)	Ar (1)	433	72	Batch	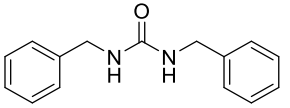 (73)	n.r.	n.r.	S8
7	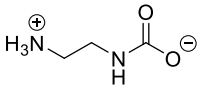 (0.57 mmol h^{-1})	CeO_2 (12)	–	EDA (–)	Air (0.1)	363	–	Fixed-bed flow	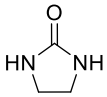 (94)[c]	>99	99.0	S9
8	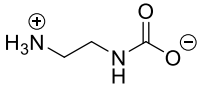 (0.41 mmol h^{-1})	1 wt% Mn-CeO_2 (12)	–	EDA (–)	Air (0.1)	363	–	Fixed-bed flow	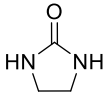 (86)[d]	92	97	S10
9	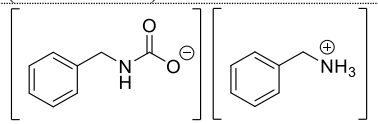 (10 mmol)	CeO_2 (2.0)	Benzylamine (100)	Methanol[b] (61)	Ar (1.0)	413	12	Batch	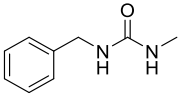 (64)	82	79	S11

10	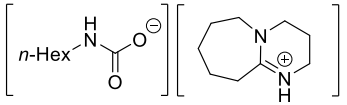 (2.0 mmol)	–	$Ti(On\text{-}Bu)_4$[b] (2.0) + *n*-BuOH[b] (6.6) + DBU (4.0)	NMP (3.0)	n.r.	423	5	Batch	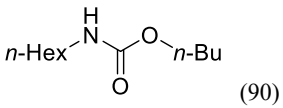 (90)	n.r.	n.r.	S12
11	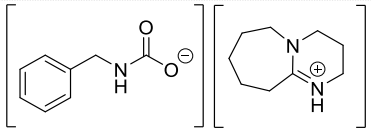 (2.0 mmol)	–	$Si(OMe)_4$[b] (7.5)	NMP (3.0)	n.r.	433	5	Batch	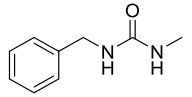 (85)	n.r.	n.r.	S13
12	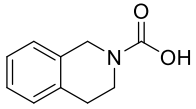 (0.375 mmol)	–	Benzyl alcohol[b] (0.563) + di-*tert*-butylazodicarboxylate (0.980) + tri-*N*-butylphosphine (0.980) + DBU (0.038)	Acetonitrile (9)	N_2 (0.1)	n.r.	1	Batch	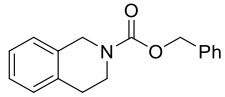 (96)	n.r.	n.r.	S14
13	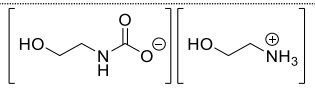 (1.0 mmol h^{-1})	CeO_2 (1.0)		2AOL (–)	Air (0.9)	413	–	Fixed-bed flow	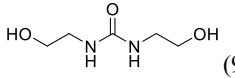 (92)[e]	93	98	This work
14	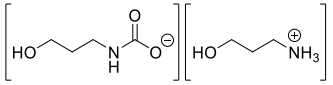 (0.39 mmol h^{-1})	CeO_2 (2.0)		3AOL (–)	Air (0.9)	413	–	Fixed-bed flow	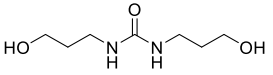 (95)[f]	93	>99	This work
15	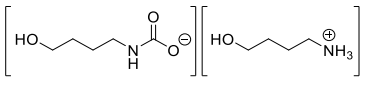 (0.060 mmol h^{-1})	CeO_2 (2.2)		4AOL (–)	Air (0.9)	413	–	Fixed-bed flow	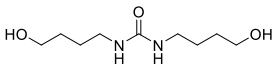 (88)[g]	52	94	This work

[a]Abbreviations: Cp = cyclopentadienyl; OTf = trifluoromethanesulfonate; NR = nanorod; O*n*-Bu = *n*-butoxy; *n*-BuOH = *n*-butanol; OMe = methoxy; DMI = 1,3-dimethyl-2-imidazolidinone; EDA = ethylenediamine; NMP = *N*-methyl-2-pyrrolidone; DBU = 1,8-diazabicyclo[5.4.0]undec-7-ene; n.r. = not reported.
[b]These compounds behaved as an alkoxy source to produce each target product.
[c]Time on stream (TOS) = 30 h; $W_{cat}/F_{EDA\text{-}CA}$ = 3.48 g_{cat} h $mmol^{-1}$.
[d]TOS = 216 h; $W_{cat}/F_{EDA\text{-}CA}$ = 4.88 g_{cat} h $mmol^{-1}$.
[e]TOS = 9 h; $W_{cat}/F_{2AOL\text{-}CA}$ = 1.0 g_{cat} h $mmol^{-1}$.
[f]TOS = 9 h; $W_{cat}/F_{3AOL\text{-}CA}$ = 5.1 g_{cat} h $mmol^{-1}$.
[g]TOS = 100 h; $W_{cat}/F_{4AOL\text{-}CA}$ = 66 g_{cat} h $mmol^{-1}$.

Table S2. Previous reports of synthesis of 2CC from 2AOL and pressurized CO_2 with homogeneous and heterogeneous catalysts.[a]

Entry	2AOL /mmol	Catalyst (mmol)	Additive (amount)	Solvent (mL)	CO_2 /MPa	Temp. /K	Time /h	2AOL conv. /%	2CC yield[b] /%	2CC sel. /%	Ref.
1	20	Ph_3SbO (2)	Molecular Sieves 3A (1 g)	Benzene (5)	5	433	3	n.r.	trace	n.r.	S15
2	60	[BMIM]Br (11.4)	K_2CO_3 (0.7 mmol)	Ethanol (4)	10	423	6	55	19	34	S16
3[b]	10	*n*-Bu_2SnO (1.0)	–	NMP (8.0)	5	453	16	87	53	61	S17
4	4.1	1,3-Dichloro-1,1,3,3-tetrabutyldistannoxane (0.017)	–	Methanol (0.20)	1.72	423	6	n.r.	55	n.r.	S18
5	0.5	Tetrabutylammonium difluorotriphenyl silicate (0.1)	–	DMSO-d_6 (0.5)	0.1	423	9	n.r.	20	n.r.	S19
6	2	np-CeO_2 (0.44)	–	Ethanol (1.9)	0.7	433	6	58	50	87	S20
7	10	CeO_2 (1.0)	–	Acetonitrile (52)	5	423	4	98	97	>99	S21
8	10	M-CeO_2-573 (1.16)	–	2-Propanol (16)	0.5	433	12	35	34	97	S22

[a]Abbreviations: Ph = phenyl; [BMIM] = 1-butyl-3-methylimidazolium cation; *n*-Bu = *n*-butyl; np = nanoparticle; NMP = *N*-methyl-2-pyrrolidone; DMSO = dimethyl sulfoxide; n.r. = not reported.
[b]Based on the mole of 2AOL used.

Table S3. Detailed information about reagents and gases used in this study.

Reagent	Detailed information
CeO_2	HS grade, Daiichi Kigenso Kagaku Kogyo, calcined at 873 K for 3 h, S_{BET} = 84 m^2 g^{-1}
Ethylenediamine	FUJIFILM Wako Pure Chemical, denoted as EDA
Butylamine	Kanto Chemical, denoted as BA
Benzylamine	FUJIFILM Wako Pure Chemical
2-Aminoethanol	Tokyo Chemical Industry, denoted as 2AOL
3-Amino-1-propanol	Tokyo Chemical Industry, denoted as 3AOL
4-Amino-1-butanol	Tokyo Chemical Industry, denoted as 4AOL
N,*N*'-Bis(2-hydroxyethyl)urea	Sigma-Aldrich, denoted as 2LU
2-Oxazolidione	Sigma-Aldrich, denoted as 2CC
1,3-Oxazinan-2-one	Sigma-Aldrich, denoted as 3CC
1,3-Oxazepan-2-one	Sigma-Aldrich, denoted as 4CC
Methyl *N*-butylcarbamate	Sigma-Aldrich
Methyl *N*-benzylcarbamate	Sigma-Aldrich
N,*N*'-Dibutylurea	FUJIFILM Wako Pure Chemical, denoted as DBU
Dibutyl carbonate	Tokyo Chemical Industry
Methanol	Kanto Chemical
Ethanol	Kanto Chemical
1-Propanol	FUJIFILM Wako Pure Chemical
2-Propanol	FUJIFILM Wako Pure Chemical
Acetonitrile	Kanto Chemical
N-Methyl-2-pyrrolidone	FUJIFILM Wako Pure Chemical, denoted as NMP
Tetrahydrofuran	FUJIFILM Wako Pure Chemical, denoted as THF
tert-Butyl alcohol	Tokyo Chemical Industry
Diethylene glycol diethyl ether	Tokyo Chemical Industry, denoted as diglyme
Deuterium oxide	Kanto Chemical
Methanol-d_4	FUJIFILM Wako Pure Chemical
Phosphate buffer solution	FUJIFILM Wako Pure Chemical, 0.1 mol/L, pH 6.8
CO_2	G1 grade (99.995%), Taiyo Nippon Sanso
$^{13}CO_2$	99 atom% ^{13}C, Sigma-Aldrich
Ar	99.99%, Taiyo Nippon Sanso
N_2	99.99%, Taiyo Nippon Sanso

Table S4. Solvent effect on the conversion of 2AOL-CA over CeO_2 catalyst in a batch reactor.[a]

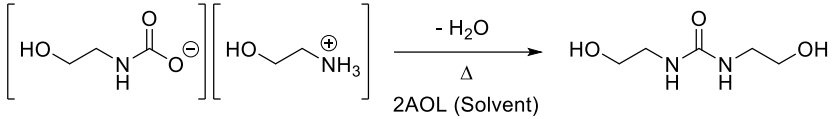

2AOL-CA (Substrate) — 2AOL (Solvent), CeO_2 — 2LU (Target product)

Entry	Solvent	Yield /%		Conv.	Sel. /%		Amount of detected compounds /mmol					Amine bal.
		2LU	2CC	/%	2LU	2CC	2AOL-CA	2AOL	2LU	2CC	Others	/%
1	Methanol	10	6.3	67	15	9.4	3.4	8.6	1.0	0.6	0	72
2	Ethanol	30	4.0	73	41	5.5	2.7	10	3.1	0.4	0	93
3	1-Propanol	28	4.4	70	40	6.3	3.0	10	2.8	0.4	0	94
4	2-Propanol	34	6.5	66	52	10	3.4	11	3.4	0.6	0	110
5	Acetonitrile	32	19	64	50	29	3.6	9.0	3.2	1.9	0.32[c]	107
6	*N*-Methyl-2-pyrrolidone (NMP)	37	11	85	43	13	1.9	6.7	4.7	1.4	0	76
7	Tetrahydrofuran (THF)	25	2.1	55	45	3.8	4.5	10	2.5	0.2	0	99
8	2-Aminoethanol (2AOL)	83	0	93	89	0	0.65	210	8.3	0	0	103
9[b]	2AOL	1	0	6	23	0	9.4	219	0.13	0	0	104

[a]Reaction conditions: 2AOL-CA 10 mmol; CeO_2 1.0 mmol; solvent 200 mmol; Ar 1.0 MPa (at r.t.); 413 K; 4 h; batch reactor (autoclave).
[b]Without CeO_2 catalyst.
[c]Acetamide was formed as a solvent-derived byproduct and quantified by GC-FID.

Table S5. Effect of granule size of CeO_2 catalyst on the conversion of 2AOL-CA in 2AOL solvent over CeO_2 catalyst at 403 K in a fixed-bed flow reactor.[a]

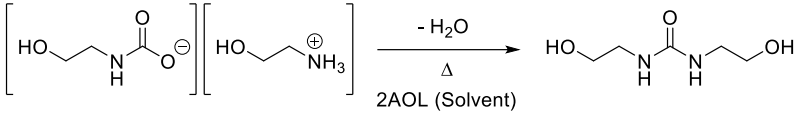

2AOL-CA (Substrate) — 2LU (Target product)

Entry	CeO_2 size /mm	W_{cat} /g	F_{sol} /mL h^{-1}	$F_{2AOL-CA}$ /mmol h^{-1}	$W_{cat}/F_{2AOL-CA}$ /g h $mmol^{-1}$	TOS /h	Yield /%		Conv. /%	Selectivity /%		Amine bal. /%	$r_{2LU+2CC}$[b] /mmol g^{-1} h^{-1}
							2LU	2CC		2LU	2CC		
1	0.25–1.0	0.30	2.4	2.0	0.15	0[c]	32	5.1	36	88	14	103	2.4
						5	32	5.6	37	87	15	104	
						7	31	4.6	35	90	13	101	
						9	32	5.2	37	87	14	103	
2	1.0–1.7	0.30	2.4	2.0	0.15	0[c]	26	4.1	30	86	14	100	2.0
						5	26	4.1	29	89	14	101	
						7	25	4.2	29	86	14	101	
						9	26	4.0	30	84	13	100	
3	1.7–2.4	0.30	2.4	2.0	0.15	0[c]	23	2.9	26	89	11	101	1.7
						5	23	2.7	26	90	10	99	
						7	24	2.9	26	89	11	102	
						9	23	3.2	26	87	12	102	
4	0.25–1.0	1.0	1.2	1.0	1.0	0[c]	80	1.4	81	99	1.7	101	0.81
						5	80	1.4	81	98	1.8	101	
						7	80	1.3	81	99	1.6	102	
						9	80	1.4	81	99	1.7	102	
5	1.0–1.7	1.0	1.2	1.0	1.0	0[c]	79	1.4	80	99	1.7	103	0.80
						5	79	1.3	80	98	1.6	103	
						7	78	1.0	79	98	1.2	102	
						9	79	1.8	79	99	2.3	103	
6	1.7–2.4	1.0	1.2	1.0	1.0	0[c]	75	1.2	76	99	1.5	101	0.75
						5	74	1.0	75	98	1.3	100	
						7	75	1.6	76	99	2.1	102	
						9	75	0.9	76	99	1.2	102	

[a]Reaction conditions: 5.0 mol% (= 8.2 wt%) 2AOL-CA in 2AOL solution; CeO_2 catalyst; 403 K; 0.9 MPa; fixed-bed flow reactor. Specific conditions are shown in the table.
[b]Total formation rate of 2LU and 2CC.
[c]The values of yield, conversion, selectivity, and amine balance at TOS = 0 h were calculated by averaging the data acquired under the steady flow.

Table S6. Effect of contact time ($W_{cat}/F_{2AOL\text{-}CA}$) on the conversion of 2AOL-CA in 2AOL solvent over CeO_2 catalyst at various temperatures in a fixed-bed flow reactor.[a]

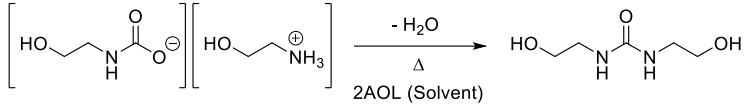

2AOL-CA (Substrate) → 2LU (Target product)

Entry	Temp. /K	W_{cat} /g	F_{sol} /mL h^{-1}	$F_{2AOL\text{-}CA}$ /mmol h^{-1}	$W_{cat}/F_{2AOL\text{-}CA}$ /g h $mmol^{-1}$	TOS /h	Yield /% 2LU	Yield /% 2CC	Conv. /%	Selectivity /% 2LU	Selectivity /% 2CC	Amine bal. /%	$r_{2LU+2CC}$[b] /mmol g^{-1} h^{-1}
1	393	0	2.4	2.0	0	0[c]	0	0	0	0	0	100	0
						5	0	0	0	0	0	101	
						7	0	0	0	0	0	100	
						9	0	0	0	0	0	101	
2	393	0.15	2.4	2.0	0.076	0[c]	6.0	3.3	9.3	64	36	101	1.2
						5	6.4	3.3	10	67	35	103	
						7	6.1	3.2	9.4	65	34	101	
						9	5.4	3.4	8.9	61	38	101	
3	393	0.30	2.4	2.0	0.15	0[c]	11	5.2	16	69	32	101	1.1
						5	12	5.2	17	70	31	102	
						7	11	5.7	16	68	34	100	
						9	11	4.7	16	71	30	102	
4	393	0.30	1.2	1.0	0.30	0[c]	23	4.7	28	82	17	100	0.92
						5	23	4.7	28	83	17	102	
						7	23	4.8	28	81	17	98	
						9	23	4.5	27	83	16	101	
5	393	0.40	1.2	1.0	0.40	0[c]	30	4.0	35	88	12	101	0.86
						5	31	4.6	35	87	13	101	
						7	31	3.8	34	90	11	101	
						9	30	3.8	34	87	11	101	
6	393	0.50	1.2	1.0	0.50	0[c]	37	3.2	41	92	7.9	101	0.82
						5	38	3.0	41	93	7.4	101	
						7	37	3.2	41	91	8.0	100	
						9	37	3.4	41	92	8.5	101	
7	393	0.60	1.2	1.0	0.60	0[c]	43	2.9	46	92	6.3	100	0.76
						5	43	3.3	46	93	7.1	102	
						7	43	2.9	47	92	6.3	98	
						9	42	2.6	46	92	5.7	99	
8	393	1.0	1.2	1.0	1.0	0[c]	53	2.5	55	96	4.6	101	0.55
						5	54	2.3	55	98	4.3	103	
						7	53	3.0	55	96	5.5	101	
						9	52	2.2	55	95	3.9	100	
9	393	1.0	0.60	0.49	2.0	0[c]	75	1.8	76	98	2.4	102	0.38
						5	75	1.9	77	98	2.5	102	
						7	74	1.7	77	97	2.2	102	
						9	74	2.0	76	98	2.7	101	
10	393	1.5	0.60	0.50	3.0	0[c]	80	1.7	80	97	2.1	101	0.27
						7	79	1.7	82	96	2.0	101	
						9	81	1.7	83	97	2.1	101	
11	393	2.0	0.48	0.40	5.0	0[c]	90	0	90	>99	0	100	0.18
						7	89	0	90	>99	0	100	

						8	90	0	90	>99	0	100		
						9	90	0	90	>99	0	101		
12	393	2.0	0.24	0.19	10	0[e]	90	0	90	>99	0	97	0.087	
						13	90	0	90	>99	0	98		
						15	89	0	90	99	0	96		
						17	92	0	91	>99	0	98		
13	403	0	2.4	2.0	0	0[e]	0	0	0	0	0	101	0	
						5	0	0	0	0	0	101		
						7	0	0	0	0	0	101		
						9	0	0	0	0	0	102		
14	403	0.15	2.4	2.0	0.074	0[e]	14	3.7	18	79	21	101	2.4	
						5	14	3.8	17	82	22	102		
						7	14	3.6	18	79	20	101		
						9	14	3.7	18	77	21	100		
15	403	0.30	2.4	2.0	0.15	0[e]	26	4.1	30	86	14	100	2.0	
						5	26	4.1	29	89	14	101		
						7	25	4.2	29	86	14	101		
						9	26	4.0	30	84	13	100		
16	403	0.50	1.2	1.0	0.50	0[e]	58	1.9	61	97	3.2	100	1.2	
						5	59	1.6	60	98	2.6	102		
						7	59	2.3	62	95	3.7	100		
						9	58	1.9	60	97	3.3	100		
17	403	1.0	1.2	1.0	1.0	0[e]	79	1.4	80	99	1.7	103	0.80	
						5	79	1.3	80	98	1.6	103		
						7	78	1.0	79	98	1.2	102		
						9	79	1.8	79	99	2.3	103		
18	403	1.0	0.60	0.50	2.0	0[e]	86	1.7	87	99	1.9	102	0.44	
						5	87	2.1	88	99	2.4	104		
						7	85	1.9	87	98	2.2	101		
						9	85	1.1	85	99	1.2	101		
19	403	1.5	0.60	0.49	3.0	0[e]	91	1.7	91	98	1.9	102	0.30	
						7	89	1.7	92	97	1.8	100		
						9	92	1.8	93	99	1.9	103		
20	403	2.0	0.48	0.40	5.0	0[e]	89	0	90	>99	0	101	0.18	
						7	89	0	90	99	0	102		
						8	88	0	89	99	0	102		
						9	88	0	89	99	0	102		
						10	93	0	92	>99	0	100		
21	403	2.0	0.24	0.20	10	0[e]	91	0	92	99	0	100	0.091	
						14	89	0	91	98	0	99		
						18	92	0	92	>99	0	100		
						20	92	0	92	>99	0	100		
22	413	0	2.4	0.64	0	0[e]	0	0	0	0	0	101	0	
						5	0	0	0	0	0	100		
						7	0	0	0	0	0	101		
						9	0	0	0	0	0	101		
23	413	0.10	3.6	3.0	0.033	0[e]	5.9	3.9	10	60	39	101	3.0	
						5	6.4	3.9	10	64	39	101		
						7	5.8	4.0	10	58	40	101		

						9	5.6	3.9	10	57	40	101		
24	413	0.15	2.4	2.0	0.074	0[e]	27	3.3	30	90	11	101	4.1	
						5	27	2.8	30	91	9.3	101		
						7	27	3.6	30	90	12	102		
						9	27	3.5	30	88	12	100		
25	413	0.30	2.4	2.0	0.15	0[e]	44	2.8	46	96	6.1	101	3.1	
						5	45	2.7	46	96	5.9	101		
						7	44	3.3	46	95	7.1	100		
						9	44	2.4	46	96	5.2	101		
26	413	0.50	1.2	1.0	0.51	0[e]	82	1.2	84	98	1.5	102	1.6	
						5	82	2.1	84	97	2.5	103		
						7	83	0	84	99	0	102		
						9	82	1.6	83	98	1.9	102		
27	413	1.0	1.7	1.4	0.71	0[e]	88	1.8	90	98	2.0	101	1.3	
						5	88	1.6	90	98	1.7	101		
						7	87	1.9	90	98	2.2	100		
						9	88	2.0	90	98	2.2	101		
28	413	1.0	1.2	1.0	1.0	0[e]	92	2.0	93	98	2.1	102	0.94	
						5	92	2.3	93	98	2.4	101		
						7	92	1.8	93	98	1.9	102		
						9	91	1.9	93	98	2.0	102		
29	413	1.0	0.60	0.49	2.0	0[e]	92	1.6	94	98	1.8	101	0.46	
						5	92	1.9	94	98	2.0	102		
						7	92	1.6	94	98	1.7	101		
						9	92	1.4	94	98	1.5	101		
30	413	2.0	0.48	0.40	5.0	0[e]	91	0	93	98	0	100	0.18	
						7	88	0	93	95	0	99		
						8	90	0	93	97	0	100		
						9	92	0	92	>99	0	100		

[a]Reaction conditions: 5.0 mol% (= 8.2 wt%) 2AOL-CA in 2AOL solution; CeO_2 with a granule size of 1.0–1.7 mm; 0.9 MPa; fixed-bed flow reactor. Specific conditions are shown in the table.
[b]Total formation rate of 2LU and 2CC.
[c]The values of yield, conversion, selectivity, and amine balance at TOS = 0 h were calculated by averaging the data acquired under the steady flow.

Table S7. Conversion of *n*CC in corresponding *n*AOL solvent at 333 K in a batch reactor (pressure-resistant glass tube).[a]

Entry	Substrate (*n*CC)	Solvent (*n*AOL)	Reaction time /min	*n*LU yield /%	*n*CC conv. /%	Amount of products /mmol					Amine bal. /%	CO_2 bal. /%
						*n*AOL-CA	*n*AOL	*n*LU	*n*CC	Others		
1	2CC	2AOL	15	7.8	18	0.03	51	0.08	0.82	0	101	93
2			30	15	25	0.03	51	0.15	0.74	0	102	92
3			45	20	28	0.02	50	0.20	0.72	0	102	94
4	3CC	3AOL	15	2.5	5.7	0.03	51	0.03	0.95	0	103	99
5			30	6.2	1.7	0.05	53	0.06	0.99	0	107	110
6			45	8.3	7.5	0.03	53	0.08	0.93	0	107	104
7[b]	4CC	4AOL	0	0	14	0.02	50	0.00	0.09	0[c]	100	107
8[b]			5	0	19	0.03	51	0.00	0.08	0[c]	102	110
9[b]			10	0	25	0.02	49	0.00	0.08	0[c]	99	91
10[b]			15	13	22	0.03	51	0.01	0.08	0[c]	103	116
11[b]			30	25	58	0.02	49	0.03	0.04	0[c]	98	84
12[b]			45	41	59	0.01	49	0.04	0.04	0[c]	98	97
13[b]			90	57	78	0.02	51	0.06	0.02	0[c]	102	98
14[b]			135	81	>99	0.02	47	0.08	0.00	0[c]	94	102

[a]Reaction conditions: *n*CC 1.0 mmol; *n*AOL 50 mmol; air 0.1 MPa; 333 K; batch reactor (pressure-resistant glass tube).

[b]Reaction conditions: 4CC 0.1 mmol; 4AOL 50 mmol; air 0.1 MPa; 333 K; batch reactor (pressure-resistant glass tube). These reactions were continuously operated, and the sampling of 0.3 g of reaction mixture was conducted at each reaction time shown in the table. The reaction results were estimated on the basis of the initial reaction solution.

[c]Neither pyrrolidine nor pyrrolidine-derived alkylcarbamic salt was detected in these experiments.

Table S8. Long-term operation of 2AOL-CA conversion in 2AOL solvent over CeO_2 catalyst at 413 K in a fixed-bed flow reactor.[a]

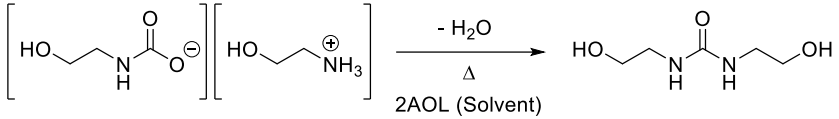

2AOL-CA (Substrate) — 2AOL (Solvent), CeO_2 — 2LU (Target product)

TOS /h	Yield /%		Conv. /%	Selectivity /%		Amine bal. /%	$r_{2AOL\text{-}CA}$[b] /mmol g^{-1} h^{-1}	S_{BET}[c] /m^2 g^{-1}
	2LU	2CC		2LU	2CC			
0[d]	88	1.8	90	98	2.0	101	1.3	
5	88	1.6	90	98	1.7	101		
7	87	1.9	90	98	2.2	100		
9	88	2.0	90	98	2.2	101		
24	87	2.0	88	98	2.2	100		
30	86	2.0	88	98	2.3	101		
48	83	1.8	84	98	2.1	100		
57	80	1.7	81	98	2.1	100		73

[a]Reaction conditions: 5.0 mol% (= 8.2 wt%) 2AOL-CA in 2AOL solution; CeO_2 with a granule size of 1.0–1.7 mm (W_{cat}) 1.0 g; F_{sol} 1.7 mL h^{-1} (= $F_{2AOL\text{-}CA}$ 1.4 mmol h^{-1}); $W_{cat}/F_{2AOL\text{-}CA}$ 0.71 g h $mmol^{-1}$; 413 K; 0.9 MPa; fixed-bed flow reactor.
[b]Conversion rate of 2AOL-CA.
[c]BET specific surface area of spent catalyst.
[d]The values of conversion, yield, selectivity, and amine balance at TOS = 0 h were calculated by extrapolating the exponentially fitted curve for the data acquired under the steady flow.

Table S9. Effect of reaction temperature on the conversion of 2AOL-CA in 2AOL solvent over CeO_2 catalyst in a fixed-bed flow reactor (for the Arrhenius plot in Fig. 5).[a]

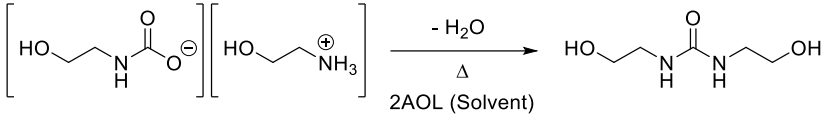

2AOL-CA (Substrate) — 2LU (Target product)

Entry	Temp. /K	W_{cat} /g	F_{sol} /mL h^{-1}	$F_{2AOL-CA}$ /mmol h^{-1}	$W_{cat}/F_{2AOL-CA}$ /g h $mmol^{-1}$	TOS /h	Yield /%		Conv. /%	Selectivity /%		Amine bal. /%	$r_{2LU+2CC}$[b] /mmol g^{-1} h^{-1}	$\ln(r_{2LU+2CC}$ /mmol g^{-1} $h^{-1})$
							2LU	2CC		2LU	2CC			
1	373	0.40	1.2	1.0	0.40	0[c]	5.0	4.8	10	50	48	100	0.24	–1.4
						5	5.2	4.7	10	50	45	100		
						7	4.8	4.9	10	51	52	101		
						9	4.9	4.7	10	50	48	101		
2	383	0.40	1.2	1.0	0.40	0[c]	14	3.8	18	76	21	102	0.45	–0.81
						5	14	3.7	18	76	20	101		
						7	14	4.1	18	75	23	101		
						9	14	3.6	18	77	20	103		
3	393	0.15	2.4	2.0	0.076	0[c]	6.0	3.3	9.3	64	36	101	1.2	0.20
						5	6.4	3.3	10	67	35	103		
						7	6.1	3.2	9.4	65	34	101		
						9	5.4	3.4	8.9	61	38	101		
4	403	0.15	2.4	2.0	0.074	0[c]	14	3.7	18	79	21	101	2.4	0.86
						5	14	3.8	17	82	22	102		
						7	14	3.6	18	79	20	101		
						9	14	3.7	18	77	21	100		
5	413	0.15	2.4	2.0	0.074	0[c]	27	3.3	30	90	11	101	4.1	1.4
						5	27	2.8	30	91	9.3	101		
						7	27	3.6	30	90	12	102		
						9	27	3.5	30	88	12	100		

[a]Reaction conditions: 5.0 mol% (= 8.2 wt%) 2AOL-CA in 2AOL solution; CeO_2 with a granule size of 1.0–1.7 mm; 0.9 MPa; fixed-bed flow reactor. Specific conditions are shown in the table.

[b]Formation rate of 2LU and 2CC.

[c]The values of conversion, yield, selectivity, and amine balance at TOS = 0 h were calculated by averaging the data acquired under the steady flow.

Table S10. Conversion of 2CC in 2AOL solvent without CeO_2 catalyst at various temperatures in a batch reactor (pressure-resistant glass tube).[a]

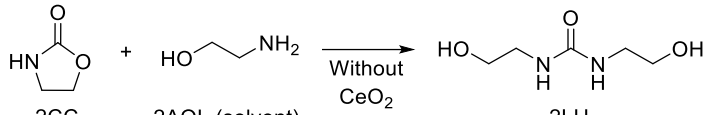

2CC 2AOL (solvent) 2LU

Entry	Temp. /K	Time /h	2LU yield /%	2CC conv. /%	2LU sel. /%	Amount of detected compounds /mmol				Amine bal. /%	C=O moiety bal.[b] /%
						2AOL-CA	2AOL	2LU	2CC		
1	323	0.25	3.7	11	32	0.024	50	0.037	0.89	102	95
2		0.50	6.6	11	60	0.040	50	0.067	0.89	102	99
3		0.75	8.8	20	43	0.034	50	0.088	0.80	101	92
4	333	0.25	7.8	18	44	0.029	51	0.078	0.82	101	93
5		0.50	15	25	58	0.025	51	0.15	0.74	102	92
6		0.75	20	28	70	0.022	50	0.20	0.72	102	94
7	343	0.17	9.5	16	60	0.045	50	0.094	0.84	102	98
8		0.33	21	32	67	0.049	51	0.21	0.68	103	94
9		0.50	32	45	71	0.033	49	0.33	0.55	99	90
10	353	0.08	7.0	16	45	0.036	50	0.070	0.84	100	95
11		0.17	21	27	75	0.041	51	0.21	0.73	103	97
12		0.25	30	41	72	0.030	50	0.29	0.58	102	91

[a]Reaction conditions: 2CC 1.0 mmol; 2AOL 100 mmol; air 0.1 MPa; 323–353 K; batch reactor (pressure-resistant glass tube).
[b]Balance of carbonyl moiety originally present in 2CC.

Table S11. Kinetic fitting analysis for the conversion of 2AOL-CA and 3AOL-CA over CeO_2 catalyst at 393 K (the fitting lines are shown in Fig. S10).

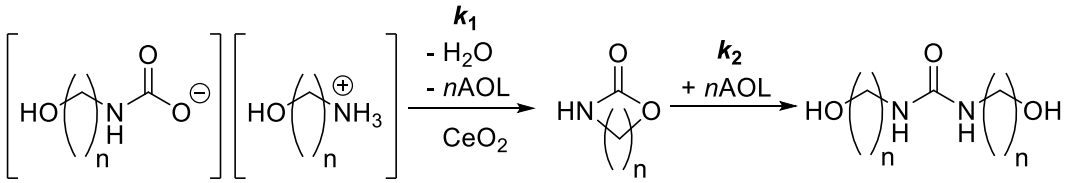

*n*AOL-CA (*n* = 2 and 3) *n*CC (*n* = 2 and 3) *n*LU (*n* = 2 and 3)

Substrate	k_1 /mmol g^{-1} h^{-1}	k_2 /mmol g^{-1} h^{-1}	t_{max} /g h $mmol^{-1}$
2AOL-CA[a]	1.0	35	0.11
3AOL-CA[b]	0.14	3.0	1.1

[a]Simulation conditions: 5.0 mol% (= 8.2 wt%) 2AOL-CA in 2AOL solution.
[b]Simulation conditions: 5.0 mol% (= 7.7 wt%) 3AOL-CA in 3AOL solution.

Table S12. Effect of concentration of 2AOL-CA on the conversion of 2AOL-CA in 2AOL solvent over CeO_2 catalyst in a fixed-bed flow reactor (for the determination of reaction order with respect to the concentration of 2AOL-CA (Fig. S11)).[a]

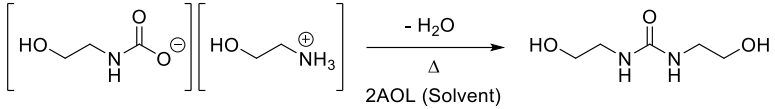

2AOL-CA (Substrate) — 2LU (Target product)

Entry	2AOL-CA conc. /M	$F_{2AOL-CA}$ /mmol h^{-1}	$W_{cat}/F_{2AOL-CA}$ /g h $mmol^{-1}$	TOS /h	Yield /%		Conv. /%	Selectivity /%		Amine bal. /%	$r_{2AOL-CA}$[b] /mmol g^{-1} h^{-1}	ln($r_{2AOL-CA}$ /mmol g^{-1} h^{-1})	ln(2AOL-CA conc. /M)
					2LU	2CC		2LU	2CC				
1	0.34	0.40	0.75	0[c]	39	7.2	46	85	16	102	0.62	–0.48	–1.1
				5	39	8.9	47	83	19	102			
				7	39	6.9	45	86	15	103			
				9	38	5.9	45	84	13	101			
2	0.50	0.60	0.50	0[c]	31	5.9	39	81	15	101	0.78	–0.25	–0.69
				5	31	5.6	39	81	14	100			
				7	31	5.9	39	81	15	102			
				9	31	6.1	38	81	16	99			
3	0.84	1.0	0.30	0[c]	23	4.7	28	82	17	100	0.93	–0.077	–0.17
				5	23	4.7	28	83	17	102			
				7	23	4.8	28	81	17	98			
				9	23	4.5	27	83	16	101			
4	1.2	1.4	0.22	0[c]	20	3.0	23	86	13	101	1.1	0.086	0.15
				5	20	3.6	24	86	15	102			
				7	20	2.8	23	87	12	101			
				9	20	2.7	24	84	12	100			

[a]Reaction conditions: 2.0–7.0 mol% (= 0.34–1.2 M) 2AOL-CA in 2AOL solution; CeO_2 with a granule size of 1.0–1.7 mm (W_{cat}) 0.30 g; F_{sol} 1.2 mL h^{-1}; 393 K; 0.9 MPa; 9 h; fixed-bed flow reactor. Specific conditions are shown in the table.
[b]Conversion rate of 2AOL-CA.
[c]The values of conversion, yield, selectivity, and amine balance at TOS = 0 h were calculated by averaging the data acquired under the steady flow.

Table S13. Effect of contact time ($W_{cat}/F_{3AOL\text{-}CA}$) on the conversion of 3AOL-CA in 3AOL solvent over CeO_2 catalyst at various temperatures in a fixed-bed flow reactor.[a]

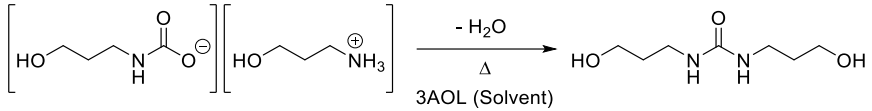

3AOL-CA (Substrate) — 3LU (Target product)

Entry	Temp. /K	W_{cat} /g	F_{sol} /mL h^{-1}	$F_{3AOL\text{-}CA}$ /mmol h^{-1}	$W_{cat}/F_{3AOL\text{-}CA}$ /g h $mmol^{-1}$	TOS /h	Yield /%			Conv. /%	Selectivity /%			Amine bal. /%	$r_{3AOL\text{-}CA}$[b] /mmol g^{-1} h^{-1}
							3LU	3CC	3LC		3LU	3CC	3LC		
1	393	0	2.4	1.6	0	0[c]	0	0	0	0	0	0	0	101	0
						5	0	0	0	0	0	0	0	101	
						7	0	0	0	0	0	0	0	101	
						9	0	0	0	0	0	0	0	101	
2	393	0.30	1.2	0.80	0.38	0[c]	5.1	1.5	0	6.7	77	22	0	102	0.18
						5	5.4	1.5	0	6.8	80	22	0	101	
						7	5.2	1.5	0	6.8	76	22	0	103	
						9	4.8	1.4	0	6.4	75	22	0	102	
3	393	1.0	0.60	0.39	2.6	0[c]	27	2.0	3.8	31	80	7.2	11	103	0.12
						5	28	1.8	3.6	32	82	7.5	10	103	
						7	27	2.2	4.0	30	80	7.5	12	103	
						9	27	2.0	3.9	30	79	6.5	12	103	
4	393	1.5	0.60	0.40	3.8	0[c]	35	1.3	4.6	41	84	3.1	11	104	0.095
						7	34	1.2	4.4	41	85	3.0	11	104	
						9	35	1.3	4.8	42	84	3.2	12	104	
5	393	2.0	0.48	0.32	6.3	0[c]	60	1.1	4.8	67	89	1.6	7.2	99	0.10
						8	60	0.94	4.5	66	91	1.4	6.8	100	
						9	60	1.1	4.8	67	90	1.6	7.1	100	
						10	59	1.3	5.2	67	87	1.9	7.7	99	
6	393	2.0	0.24	0.16	13	0[c]	80	1.2	0	81	99	1.5	0	99	0.064
						17	80	0.70	0	81	99	0.87	0	99	
						19	80	1.5	0	81	99	1.8	0	99	
						21	79	1.5	0	80	99	1.8	0	100	
7	393	2.2	0.18	0.12	19	0[c]	85	0.74	0	87	99	0.86	0	100	0.046
						28	85	0.61	0	87	98	0.71	0	101	
						30	85	0.97	0	87	99	1.1	0	100	
						32	85	0.65	0	86	99	0.75	0	100	
8	393	2.2	0.12	0.18	27	0[c]	91	0	0	90	>99	0	0	100	0.033
						37	91	0	0	91	>99	0	0	100	
						39	91	0	0	91	>99	0	0	100	
						45	91	0	0	90	>99	0	0	100	
9	393	2.2	0.060	0.040	55	0[c]	94	0	0	94	>99	0	0	101	0.017
						74	94	0	0	94	>99	0	0	101	
						76	94	0	0	94	>99	0	0	101	
						78	94	0	0	94	>99	0	0	100	
10	403	0	2.4	1.6	0	0[c]	0	0	0	0	0	0	0	101	0
						5	0	0	0	0	0	0	0	102	
						7	0	0	0	0	0	0	0	101	
						9	0	0	0	0	0	0	0	100	

11	403	0.30	1.2	0.79	0.38	0[c]	20	0	2.5	22	88	0	11	100	0.52
						5	20	0	2.2	23	89	0	10	99	
						7	20	0	2.6	22	89	0	12	100	
						9	19	0	2.7	23	85	0	12	100	
12	403	1.0	1.2	0.78	1.3	0[c]	37	2.8	5.5	46	80	6.1	12	102	0.31
						5	37	3.3	4.9	46	81	7.2	11	103	
						7	36	2.8	5.8	46	79	6.2	13	101	
						9	37	2.3	5.9	47	80	5.0	13	103	
13	403	1.0	0.60	0.39	2.6	0[c]	61	1.3	6.4	69	88	1.9	9.2	103	0.24
						5	61	1.1	7.1	71	87	1.6	10	102	
						7	61	1.4	6.2	69	88	2.0	9.0	103	
						9	61	1.5	5.8	68	89	2.2	8.5	103	
14	403	1.5	0.60	0.39	3.8	0[c]	65	1.4	3.3	70	93	1.9	4.7	102	0.17
						7	66	1.5	3.5	71	92	2.1	4.9	102	
						9	64	1.2	3.1	69	93	1.8	4.5	101	
15	403	2.0	0.48	0.32	6.3	0[c]	83	0	2.0	86	97	0	2.4	100	0.13
						8	83	0	2.4	87	96	0	2.7	100	
						9	83	0	1.9	85	97	0	2.2	99	
						10	83	0	1.9	85	97	0	2.2	100	
16	403	2.0	0.24	0.16	13	0[c]	92	0	0.88	93	99	0	0.95	100	0.073
						16	91	0	0.56	92	99	0	0.61	100	
						18	92	0	0.94	93	99	0	1.0	99	
						20	92	0	1.1	93	99	0	1.2	100	
17	403	2.2	0.18	0.12	18	0[c]	94	0	0	94	>99	0	0	100	0.051
						28	94	0	0	95	99	0	0	100	
						30	94	0	0	94	>99	0	0	100	
						32	94	0	0	94	>99	0	0	100	
18	413	0	2.4	0.53	0	0[c]	0	0	0	0	0	0	0	100	0
						5	0	0	0	0	0	0	0	100	
						7	0	0	0	0	0	0	0	100	
						9	0	0	0	0	0	0	0	100	
19	413	0.30	1.2	0.80	0.38	0[c]	33	0	3.9	37	87	0	10	102	0.87
						5	33	0	3.5	38	89	0	9.4	101	
						7	33	0	3.9	37	88	0	11	103	
						9	32	0	4.3	37	86	0	12	102	
20	413	0.60	1.2	0.77	0.78	0[c]	53	1.9	7.5	63	83	3.0	12	103	0.70
						5	53	1.9	7.7	63	83	3.0	12	104	
						7	53	1.9	7.3	63	84	2.9	12	103	
						9	52	1.9	7.6	63	83	3.1	12	104	
21	413	1.0	1.2	0.79	1.3	0[c]	70	1.6	8.2	80	87	2.0	10	101	0.56
						5	69	1.5	8.5	81	85	1.9	11	101	
						7	70	1.7	8.1	80	87	2.1	10	102	
						9	71	1.7	7.9	80	89	2.1	10	101	
22	413	1.0	0.60	0.40	2.5	0[c]	82	1.4	2.0	86	96	1.6	2.3	102	0.33
						5	82	1.5	1.8	85	96	1.7	2.1	103	
						7	82	1.2	2.3	86	95	1.4	2.6	100	
						9	82	1.5	2.0	87	95	1.7	2.3	103	
23	413	1.5	0.60	0.36	4.1	0[c]	90	0	0	85	>99	0	0	103	0.22
						7	90	0	0	86	>99	0	0	103	

						9	89	0	0	85	>99	0	0	103	
24	413	2.0	0.60	0.39	5.1	0[c]	95	0	0	93	>99	0	0	102	0.19
						5	89	0	0	94	95	0	0	103	
						7	95	0	0	93	>99	0	0	102	
						9	95	0	0	93	>99	0	0	102	
25	413	2.0	0.24	0.16	13	0[c]	95	0	0	95	>99	0	0	100	0.075
						18	95	0	0	95	>99	0	0	100	
						20	95	0	0	95	>99	0	0	100	
						22	95	0	0	95	>99	0	0	100	
26	413	2.2	0.18	0.12	19	0[c]	95	0	0	95	>99	0	0	100	0.051
						28	95	0	0	95	>99	0	0	101	
						30	95	0	0	95	>99	0	0	100	
						32	96	0	0	96	>99	0	0	100	

[a]Reaction conditions: 5.0 mol% (= 7.7 wt%) 3AOL-CA in 3AOL solution; CeO_2 with a granule size of 1.0–1.7 mm; 0.9 MPa; fixed-bed flow reactor. Specific conditions are shown in the table.
[b]Total formation rate of 3LU and 3CC.
[c]The values of conversion, yield, selectivity, and amine balance at TOS = 0 h were calculated by averaging the data acquired under the steady flow.

Table S14. Long-term operation of 3AOL-CA conversion in 3AOL solvent over CeO_2 catalyst at 413 K in a fixed-bed flow reactor.[a]

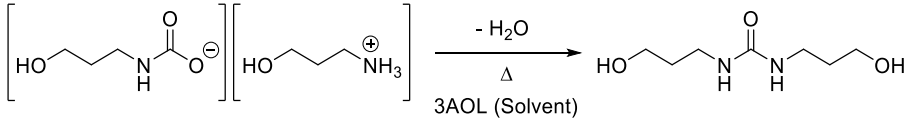

3AOL-CA (Substrate) — 3LU (Target product)

TOS /h	Yield /%			Conv.	Selectivity /%			Amine bal.	$r_{3AOL-CA}$[b]	S_{BET}[c]
	3LU	3CC	3LC	/%	3LU	3CC	3LC	/%	/mmol g^{-1} h^{-1}	/m^2 g^{-1}
0[d]	78	1.5	3.3	85	92	1.8	3.8	102	0.20	
5	78	1.7	3.3	85	92	2.0	3.9	101		
7	78	1.6	3.0	85	92	1.9	3.5	102		
9	78	1.2	3.5	85	92	1.4	4.1	102		
24	78	2.0	3.3	84	92	2.4	3.9	103		
30	77	1.9	3.6	84	92	2.3	4.3	101		
48	75	1.8	3.1	81	92	2.2	3.8	102		
57	74	1.5	3.3	80	93	1.9	4.2	101		
122	72	1.8	3.5	78	93	2.3	4.4	101		
146	70	2.4	3.1	76	92	3.1	4.1	101		
194	66	2.1	3.7	72	92	2.9	5.1	99		72

[a]Reaction conditions: 5.0 mol% (= 7.7 wt%) 3AOL-CA in 3AOL solution; CeO_2 with a granule size of 1.0–1.7 mm (W_{cat}) 1.0 g; F_{sol} 0.60 mL h^{-1} (= $F_{3AOL-CA}$ 0.25 mmol h^{-1}); $W_{cat}/F_{3AOL-CA}$ 4.0 g h $mmol^{-1}$; 413 K; 0.9 MPa; fixed-bed flow reactor.
[b]Conversion rate of 3AOL-CA.
[c]BET specific surface area of spent catalyst.
[d]The values of conversion, yield, selectivity, and amine balance at TOS = 0 h were calculated by extrapolating the exponentially fitted curve for the data acquired under the steady flow.

Table S15. Effect of reaction temperature on the conversion of 3AOL-CA in 3AOL solvent over CeO_2 catalyst in a fixed-bed flow reactor (for the Arrhenius plot in Fig. 5).[a]

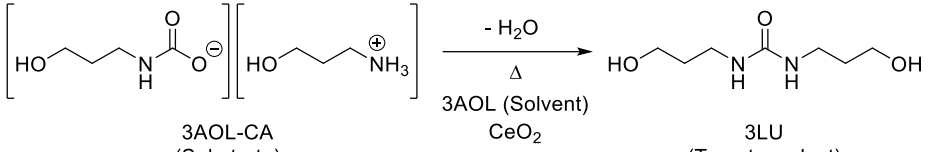

Entry	Temp. /K	W_{cat} /g	F_{sol} /mL h^{-1}	$F_{3AOL-CA}$ /mmol h^{-1}	$W_{cat}/F_{3AOL-CA}$ /g h $mmol^{-1}$	TOS /h	Yield /% 3LU	3CC	3LC	Conv. /%	Selectivity /% 3LU	3CC	3LC	Amine bal. /%	$r_{3LU+3CC}$[b] /mmol g^{-1} h^{-1}	$\ln(r_{3LU+3CC}$ /mmol g^{-1} $h^{-1})$
1	373	1.0	0.60	0.39	2.5	0[c]	6.6	1.8	0	8.7	75	20	0	102	0.033	–3.4
						5	7.1	1.5	0	10	74	16	0	102		
						7	6.1	1.8	0	8.4	73	22	0	101		
						9	6.5	1.9	0	8.3	79	23	0	102		
2	383	1.0	0.60	0.39	2.6	0[c]	17	1.8	2.7	22	79	8.4	13	103	0.075	–2.6
						5	18	1.8	3.1	22	80	8.2	14	104		
						7	18	1.8	2.4	22	82	8.5	11	103		
						9	17	1.8	2.7	22	77	8.5	13	103		
3	393	0.30	1.2	0.80	0.38	0[c]	5.1	1.5	0	6.7	77	22	0	102	0.18	–1.7
						5	5.4	1.5	0	6.8	80	22	0	101		
						7	5.2	1.5	0	6.8	76	22	0	103		
						9	4.8	1.4	0	6.4	75	22	0	102		
4	403	0.30	1.2	0.79	0.38	0[c]	20	0	2.5	22	88	0	11	100	0.52	–0.65
						5	20	0	2.2	23	89	0	10	99		
						7	20	0	2.6	22	89	0	12	100		
						9	19	0	2.7	23	85	0	12	100		
5	413	0.30	1.2	0.78	0.38	0[c]	33	0	3.9	37	87	0	10	102	0.85	–0.17
						5	33	0	3.5	38	89	0	9.4	101		
						7	33	0	3.9	37	88	0	11	103		
						9	32	0	4.3	37	86	0	12	102		

[a]Reaction conditions: 5.0 mol% (=7.7wt%) 3AOL-CA in 3AOL solution; CeO_2 with a granule size of 1.0–1.7 mm; 0.9 MPa; fixed-bed flow reactor. Specific conditions are shown in the table.
[b]Total formation rate of 3LU and 3CC.
[c]The values of conversion, yield, selectivity, and amine balance at TOS = 0 h were calculated by averaging the data acquired under the steady flow.

Table S16. Effect of concentration of 3AOL-CA on the conversion of 3AOL-CA in 3AOL solvent over CeO_2 catalyst in a fixed-bed flow reactor (for the determination of reaction order with respect to the concentration of 3AOL-CA (Fig. S11)).[a]

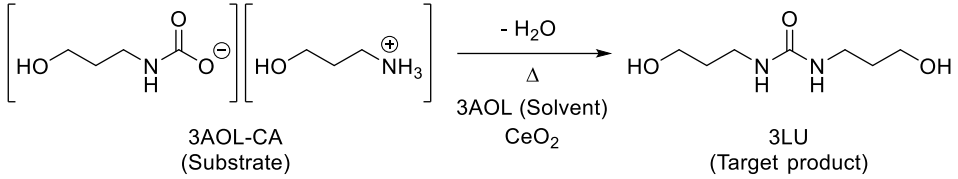

3AOL-CA (Substrate) — 3LU (Target product)

Entry	3AOL-CA conc. /M	$F_{3AOL-CA}$ /mmol h^{-1}	$W_{cat}/F_{3AOL-CA}$ /g h $mmol^{-1}$	TOS /h	Yield /%			Conv. /%	Selectivity /%			Amine bal. /%	$r_{3AOL-CA}$[b] /mmol g^{-1} h^{-1}	ln($r_{3AOL-CA}$ /mmol g^{-1} h^{-1})	ln(3AOL-CA conc. /M)
					3LU	3CC	3LC		3LU	3CC	3LC				
1	0.91	1.1	0.91	0[c]	20	1.5	2.3	24	83	6.3	10	102	0.27	–1.3	–0.089
				5	20	1.4	3.0	25	81	5.4	12	102			
				7	20	1.6	2.1	24	83	6.5	8.6	102			
				9	20	1.6	2.0	24	85	6.8	8.3	102			
2	0.66	0.79	1.3	0[c]	24	2.4	3.6	31	78	7.8	12	103	0.24	–1.4	–0.42
				5	24	2.5	3.7	31	77	8.1	12	101			
				7	24	2.4	3.7	31	78	7.7	12	103			
				9	24	2.2	3.4	30	80	7.4	12	104			
3	0.39	0.47	2.1	0[c]	28	3.4	3.7	35	80	10	10	103	0.17	–1.8	–0.93
				5	29	2.8	3.8	35	81	7.9	11	103			
				7	28	3.4	4.0	36	79	10	11	103			
				9	27	3.8	3.2	34	80	11	9.3	102			
4	0.26	0.32	3.2	0[c]	31	4.8	5.4	42	74	12	13	100	0.13	–2.0	–1.3
				5	30	4.8	5.4	41	74	12	13	98			
				7	31	5.0	6.1	43	73	11	14	100			
				9	31	4.7	4.8	41	76	12	12	101			

[a]Reaction conditions: 2.0–7.0 mol% (= 0.26–0.91 M) 3AOL-CA in 3AOL solution; CeO_2 with a granule size of 1.0–1.7 mm (W_{cat}) 1.0 g; F_{sol} 1.2 mL h^{-1}; 393 K; 0.9 MPa; 9 h; fixed-bed flow reactor. Specific conditions are shown in the table.

[b]Conversion rate of 3AOL-CA.

[c]The values of conversion, yield, selectivity, and amine balance at TOS = 0 h were calculated by averaging the data acquired under the steady flow.

Table S17. Effect of contact time ($W_{cat}/F_{4AOL\text{-}CA}$) on the conversion of 4AOL-CA in 4AOL solvent over CeO_2 catalyst at various temperatures in a fixed-bed flow reactor.[a]

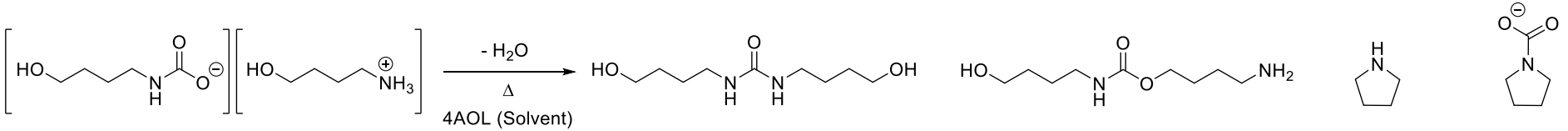

4AOL-CA (Substrate) | 4LU (Target product) | 4LC | Pyrrolidine | Pyrrolidine-derived alkylcarbamic salt

Entry	Temp. /K	W_{cat} /g	F_{sol} /mL h^{-1}	$F_{4AOL\text{-}CA}$ /mmol h^{-1}	$W_{cat}/F_{4AOL\text{-}CA}$ /g h $mmol^{-1}$	TOS /h	Yield /%		Amount of products /μmol h^{-1}				(Pyrrolidine +derivative) /(4LU+4LC)[b]	Conv. /%	Selectivity /%		Amine bal. /%	r_{4LU}[c] /mmol g^{-1} h^{-1}
							4LU	4LC	4LU	4LC	Pyrrolidine	Pyrrolidine-derived alkylcarbamic salt			4LU	4LC		
1	393	1.0	0.60	0.32	3.1	0[d]	4.3	9.6	14	31	7.0	0	0.16	24	31	69	99	0.014
						7	4.4	9.2	14	30	7.1	0	0.16	22	32	68	98	
						8	3.9	10	13	33	7.5	0	0.16	26	28	72	100	
						9	4.7	10	15	31	6.6	0	0.14	23	33	67	100	
2	393	2.2	0.12	0.064	34	0[d]	19	6.7	12	4.4	6.4	0.61	0.42	24	82	16	99	0.0056
						42	19	7.1	13	4.7	6.0	0.63	0.38	25	81	17	98	
						44	18	6.6	12	4.3	6.5	0.69	0.44	23	81	16	99	
						46	20	6.5	13	4.2	6.6	0.50	0.42	23	83	16	100	
3	393	2.2	0.060	0.033	68	0[d]	38	7.4	12	2.4	6.5	0.56	0.47	30	79	15	101	0.0056
						96	36	7.3	12	2.5	6.0	0.37	0.44	33	80	16	100	
						98	39	7.7	13	2.5	6.4	0.64	0.46	31	78	16	103	
						100	38	7.1	12	2.3	6.6	0.48	0.49	29	80	15	101	
4	403	1.0	0.60	0.32	3.1	0[d]	5.9	5.9	19	19	11	1.3	0.32	17	49	49	101	0.019
						7	6.0	5.4	20	17	11	0.75	0.30	17	52	47	100	
						8	6.1	5.5	19	17	10	1.9	0.33	17	51	46	102	
						9	5.5	6.8	18	22	11	1.1	0.32	17	44	55	100	
5	403	2.2	0.12	0.063	35	0[d]	29	4.0	19	2.5	11	1.3	0.57	20	83	11	99	0.0084
						42	29	3.8	19	2.4	11	1.1	0.58	19	84	11	100	
						44	29	3.4	19	2.2	11	1.3	0.60	18	84	10	99	
						46	30	4.7	19	3.0	10	1.4	0.53	22	81	13	99	
6	403	2.2	0.060	0.031	70	0[d]	61	2.3	20	0.76	9.1	0.58	0.47	36	92	3.5	98	0.0087
						96	62	2.5	20	0.80	9.3	0.55	0.48	34	92	3.7	99	
						98	60	2.3	19	0.74	9.0	0.53	0.47	38	92	3.5	99	
						100	60	2.2	19	0.73	8.9	0.66	0.47	36	92	3.4	98	
7	413	0	0.60	0.32	0	0[d]	0	0	0	0	0	0	0	0	0	0	102	0
						7	0	0	0	0	0	0	0	0	0	0	101	
						8	0	0	0	0	0	0	0	0	0	0	102	
						9	0	0	0	0	0	0	0	0	0	0	103	
8	413	1.0	0.60	0.32	3.2	0[d]	29	9.3	92	29	47	5.3	0.43	37	73	23	101	0.091
						7	29	8.8	91	28	46	6.0	0.44	32	73	22	102	

						8	29	9.2	93	29	48	5.0	0.43	38	73	23	101		
						9	29	9.8	91	31	45	4.9	0.41	42	72	25	101		
9	413	2.2	0.12	0.061	36	0[d]	75	0	45	0	17	2.8	0.45	42	94	0	102	0.021	
						42	75	0	45	0	17	2.9	0.44	42	94	0	103		
						44	74	0	45	0	17	2.7	0.44	44	94	0	100		
						46	75	0	45	0	18	2.9	0.47	40	94	0	102		
10	413	2.2	0.060	0.034	66	0[d]	88	0	31	0	9.2	2.1	0.37	52	94	0	97	0.013	
						96	87	0	31	0	9.2	2.1	0.37	53	94	0	97		
						98	88	0	31	0	9.3	1.8	0.36	53	93	0	97		
						100	88	0	31	0	9.2	2.3	0.38	51	94	0	97		

[a]Reaction conditions: 5.0 mol% (= 7.2 wt%) 4AOL-CA in 4AOL solution; CeO_2 with a granule size of 1.0–1.7 mm; 0.9 MPa; fixed-bed flow reactor. Specific conditions are shown in the table.
[b]Ratio of the amount of products.
[c]Formation rate of 4LU.
[d]The values of conversion, yield, selectivity, and amine balance at TOS = 0 h were calculated by averaging the data acquired under the steady flow.

Table S18. Control reactions of 4AOL in the presence/absence of 4AOL-CA and CeO_2.[a]

Entry	4AOL-CA conc. /mol%	CeO_2 /g	F_{sol} /mmol h^{-1}	$F_{4AOL\text{-}CA}$ /mmol h^{-1}	$W_{cat}/F_{4AOL\text{-}CA}$ /g h $mmol^{-1}$	TOS /h	Yield /%		Amount of byproducts /μmol h^{-1}				(Pyrrolidine +derivative) /(4LU+4LC)[b]	Conv. /%	Selectivity /%		Amine bal. /%	r_{4LU}[c] /mmol g^{-1} h^{-1}
							4LU	4LC	4LU	4LC	Pyrrolidine	Pyrrolidine-derived alkylcarbamic salt			4LU	4LC		
1	5.0	1.0	0.60	0.32	3.2	0[d]	29	9.3	92	29	47	5.3	0.43	37	73	23	101	0.091
						7	29	8.8	91	28	46	6.0	0.44	32	73	22	102	
						8	29	9.2	93	29	48	5.0	0.43	38	73	23	101	
						9	29	9.8	91	31	45	4.9	0.41	42	72	25	101	
2	0	1.0	0.60	0	0	0[d]	0	0	0	0	0	0	0	0	0	0	102	0
						7	0	0	0	0	0	0	0	0	0	0	100	
						8	0	0	0	0	0	0	0	0	0	0	102	
						9	0	0	0	0	0	0	0	0	0	0	102	
3	5.0	0	0.60	0.32	0	0[d]	0	0	0	0	0	0	0	0	0	0	102	0
						7	0	0	0	0	0	0	0	0	0	0	101	
						8	0	0	0	0	0	0	0	0	0	0	102	
						9	0	0	0	0	0	0	0	0	0	0	103	

[a]Reaction conditions: 0 or 5.0 mol% (= 7.2 wt%) 4AOL-CA in 4AOL solution; F_{sol} 0.60 mL h^{-1}; CeO_2 with a granule size of 1.0–1.7 mm (W_{cat}) 1.0 g; 413 K; 0.9 MPa; fixed-bed flow reactor. Specific conditions are shown in the table.
[b]Ratio of the amount of products.
[c]Formation rate of 4LU.
[d]The values of conversion, yield, selectivity, and amine balance at TOS = 0 h were calculated by averaging the data acquired under the steady flow.

Table S19. Effect of additive (either water or pyrrolidine) on the conversion of 4AOL-CA in 4AOL solvent over CeO_2 catalyst at 413 K in a fixed-bed flow-type reactor.[a]

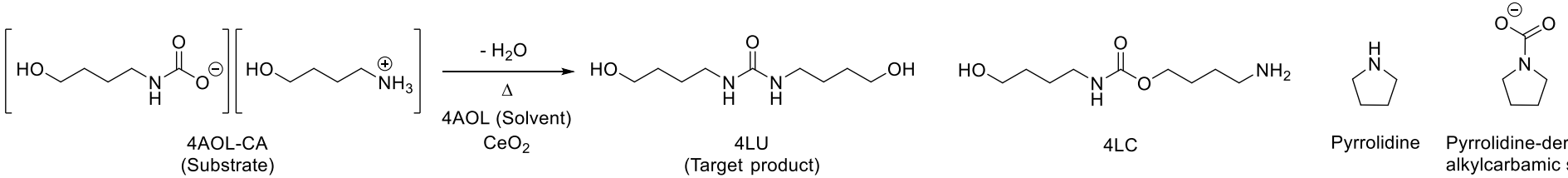

Entry	Additive	TOS /h	Yield /%		Amount of byproducts /μmol h^{-1}				(Pyrrolidine +derivative) /(4LU+4LC)[b]	Conv. /%	Selectivity /%		Amine bal. /%	r_{4LU}[c] /mmol g^{-1} h^{-1}
			4LU	4LC	4LU	4LC	Pyrrolidine	Pyrrolidine-derived alkylcarbamic salt			4LU	4LC		
1	None	0[d]	29	9.3	91	29	47	5.3	0.43	37	76	24	101	0.091
		7	29	8.8	93	28	46	6.0	0.44	32	77	23	102	
		8	29	9.2	91	29	48	5.0	0.44	38	76	24	101	
		9	29	10	91	31	45	4.9	0.41	42	75	25	101	
2	Pyrrolidine	0[d]	28	8.4	91	29	56 (39)[e]	7.4[e]	0.56 (0.41)[f]	30	77	23	102	0.087
		7	27	8.6	91	28	58 (41)[e]	7.0[e]	0.58 (0.43)[f]	31	76	24	102	
		8	28	7.9	93	29	54 (37)[e]	7.2[e]	0.56 (0.40)[f]	29	78	22	104	
		9	28	8.8	91	31	56 (39)[e]	7.9[e]	0.55 (0.40)[f]	30	76	24	100	
3	H_2O	0[d]	20	7.0	63	22	33	3.9	0.44	25	74	26	102	0.064
		7	21	7.0	64	22	32	3.6	0.42	25	73	25	103	
		8	20	6.9	62	21	33	3.6	0.44	25	74	26	102	
		9	20	7.2	63	23	34	4.6	0.45	25	73	27	100	

[a]Reaction conditions: 5.0 mol% (= 7.2 wt%) 4AOL-CA and 0.3 mol% additive (either pyrrolidine or H_2O) in 4AOL solution; F_{sol} 0.60 mL h^{-1} (= $F_{4AOL\text{-}CA}$ 0.32 mmol h^{-1}); CeO_2 with a granule size of 1.0–1.7 mm (W_{cat}) 1.0 g; $W_{cat}/F_{4AOL\text{-}CA}$ 3.2 g h $mmol^{-1}$; 413 K; 0.9 MPa; TOS 9 h.
[b]Ratio of the amount of products.
[c]Formation rate of 4LU.
[d]The values of conversion, yield, selectivity, and amine balance at TOS = 0 h were calculated by averaging the data acquired under the steady flow.
[e]The values outside and inside parentheses are the detected amount and corrected amount via subtraction of the amount of pyrrolidine that was intentionally added into the reaction solution.
[f]The values should include the amount of product derived from pyrrolidine that was intentionally added into the reaction solution.

Table S20. Effect of reaction temperature on the conversion of 4AOL-CA in 4AOL solvent over CeO_2 catalyst in a fixed-bed flow reactor (for the Arrhenius plot in Fig. 5).[a]

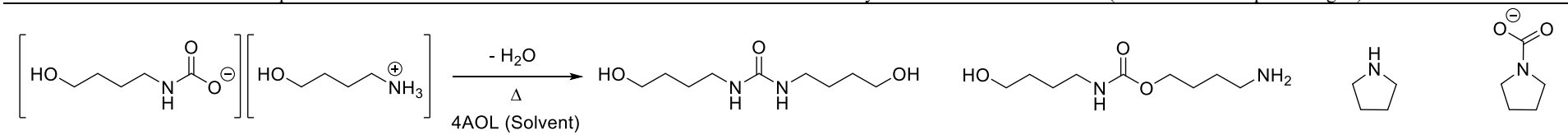

4AOL-CA (Substrate) | 4LU (Target product) | 4LC | Pyrrolidine | Pyrrolidine-derived alkylcarbamic salt

Entry	Temp. /K	W_{cat} /g	F_{sol} /mL h^{-1}	$F_{4AOL-CA}$ /mmol h^{-1}	W_{cat} /$F_{4AOL-CA}$/g h $mmol^{-1}$	TOS /h	Yield /%		Amount of byproducts /μmol h^{-1}				(Pyrrolidine +derivative) /(4LU+4LC)[b]	Conv. /%	Selectivity /%		Amine bal. /%	r_{4LU}[c] /mmol g^{-1} h^{-1}	ln(r_{4LU} /mmol g^{-1} h^{-1})
							4LU	4LC	4LU	4LC	Pyrrolidine	Pyrrolidine-derived alkylcarbamic salt			4LU	4LC			
1	373	2.2	0.12	0.063	35	0[d]	2.7	6.3	1.7	4.1	0.59	0	0.10	10	30	70	97	0.00077	–7.2
						50	2.1	6.9	1.4	4.5	0.64	0	0.11	10	23	77	97		
						52	3.4	5.8	2.2	3.7	0.57	0	0.10	10	37	63	97		
						54	2.6	6.3	1.7	4.1	0.57	0	0.10	11	29	71	98		
2	383	2.2	0.12	0.065	33	0[d]	4.9	3.9	3.4	2.7	0.95	0.18	0.18	15	54	43	96	0.0016	–6.4
						50	4.4	3.8	3.0	2.6	0.92	0.12	0.18	16	52	46	96		
						52	5.3	4.5	3.7	3.1	0.75	0.44	0.17	16	51	43	95		
						54	5.1	3.5	3.5	2.4	1.2	0	0.20	13	60	40	96		
3	393	2.2	0.12	0.064	34	0[d]	19	6.7	12	4.4	6.4	0.61	0.42	24	82	16	99	0.0056	–5.2
						42	19	7.1	13	4.7	6.0	0.64	0.39	25	81	17	98		
						44	18	6.6	12	4.3	6.6	0.69	0.44	23	81	16	99		
						46	20	6.5	13	4.2	6.6	0.50	0.42	23	83	16	100		
4	403	1.0	0.60	0.32	3.1	0[d]	5.9	5.9	19	19	11	1.3	0.32	11	49	49	101	0.019	–4.0
						7	6.0	5.4	20	17	11	0.75	0.30	13	52	47	100		
						8	6.1	5.5	19	17	10	1.9	0.33	9.5	51	46	102		
						9	5.5	6.8	18	22	11	1.1	0.32	12	44	55	100		
5	413	1.0	0.60	0.32	3.2	0[d]	29	9.3	92	29	47	5.3	0.43	37	73	23	101	0.091	–2.4
						7	29	8.8	91	28	46	6.0	0.44	32	73	22	102		
						8	29	9.2	93	29	48	5.0	0.44	38	73	23	101		
						9	29	9.8	91	31	46	5.0	0.41	42	72	25	101		

[a]Reaction conditions: 5.0 mol% (=7.2 wt%) 4AOL-CA in 4AOL solution; CeO_2 with a granule size of 1.0–1.7 mm; 0.9 MPa; fixed-bed flow reactor. Specific conditions are shown in the table.
[b]Ratio of the amount of products.
[c]Formation rate of 4LU.
[d]The values of yield, conversion, selectivity, and amine balance at TOS = 0 h were calculated by averaging the data acquired under the steady flow.

Table S21. Effect of concentration of 4AOL-CA on the conversion of 4AOL-CA in 4AOL solvent over CeO_2 catalyst in a fixed-bed flow reactor (for the determination of reaction order with respect to the concentration of 4AOL-CA (Fig. S11).[a]

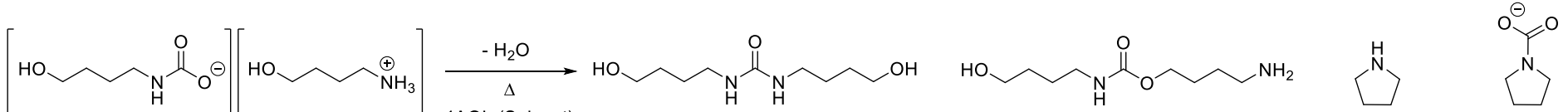

4AOL-CA (Substrate) | 4LU (Target product) | 4LC | Pyrrolidine | Pyrrolidine-derived alkylcarbamic salt

Entry	4AOL-CA conc. /M	$F_{4AOL-CA}$ /mmol h^{-1}	$W_{cat}/F_{4AOL-CA}$ /g h $mmol^{-1}$	TOS /h	Yield /%		Amount of byproducts /μmol h^{-1}				(Pyrrolidine +derivative) /(4LU+4LC)[b]	Conv. /%	Selectivity /%		Amine bal. /%	r_{4LU}[c] /mmol g^{-1} h^{-1}	ln($r_{4AOL-CA}$ /mmol g^{-1} h^{-1})	ln(4AOL-CA conc. /M)
					4LU	4LC	4LU	4LC	Pyrrolidine	Pyrrolidine-derived alkylcarbamic salt			4LU	4LC				
1	0.73	0.088	25	0[d]	17	6.8	17	6.8	8.7	0.94	0.45	19	67	26	99	0.0074	–4.9	–0.31
				36	16	6.7	16	6.7	9.0	1.0	0.48	19	66	27	99			
				38	16	6.7	16	6.7	8.9	1.0	0.49	18	65	27	99			
				40	19	6.9	19	6.9	8.3	0.85	0.39	19	69	25	99			
2	0.54	0.064	34	0[d]	19	6.7	19	6.7	6.4	0.61	0.42	24	82	16	99	0.0069	–5.0	–0.62
				42	19	7.1	19	7.1	6.0	0.64	0.39	25	81	17	98			
				44	18	6.6	18	6.6	6.6	0.69	0.44	23	81	16	99			
				46	20	6.5	20	6.5	6.6	0.50	0.42	23	83	16	100			
3	0.31	0.037	59	0[d]	13	5.5	13	5.5	2.8	0.18	0.42	14	67	29	95	0.0023	–6.1	–1.2
				66	12	6.5	12	6.5	2.7	0.21	0.40	15	62	33	95			
				68	13	4.4	13	4.4	2.8	0.16	0.42	12	72	24	96			
				70	12	5.4	12	5.4	2.8	0.18	0.44	14	66	30	94			
4	0.20	0.024	92	0[d]	16	5.3	16	5.3	1.9	0.060	0.39	19	74	25	98	0.0013	–6.6	–1.6
				96	15	5.2	16	5.2	2.1	0	0.39	19	76	24	97			
				98	16	6.3	15	6.3	1.7	0.18	0.37	22	67	28	97			
				100	16	4.6	16	4.6	2.0	0	0.41	15	78	22	100			

[a]Reaction conditions: 2.0–7.0 mol% (= 0.20–0.73 M) 4AOL-CA in 4AOL solution; CeO_2 with a granule size of 1.0–1.7 mm (W_{cat}) 2.2 g; F_{sol} 0.12 mL h^{-1}; 393 K; 0.9 MPa; fixed-bed flow reactor. Specific conditions are shown in the table.
[b]Ratio of the amount of products.
[c]Conversion rate of 4AOL-CA.
[d]The values of conversion, yield, selectivity, and amine balance at TOS = 0 h were calculated by averaging the data acquired under the steady flow.

Table S22. Effect of contact time ($W_{cat}/F_{EDA\text{-}CA}$) on the conversion of EDA-CA in EDA solvent over CeO_2 catalyst at various temperatures in a fixed-bed flow reactor.[a]

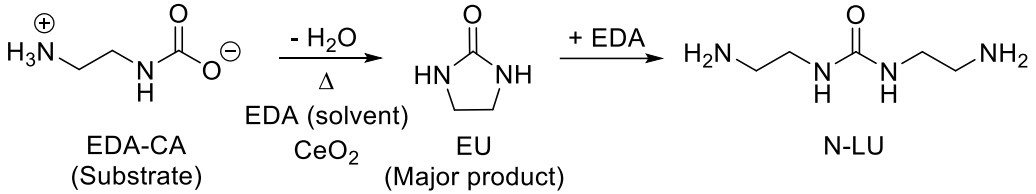

Entry	Temp. /K	W_{cat} /g	F_{Sol} /mL h^{-1}	$F_{EDA\text{-}CA}$ /mmol h^{-1}	$W_{cat}/F_{EDA\text{-}CA}$ /g h $mmol^{-1}$	TOS /h	Yield /% N-LU	Yield /% EU	Conv. /%	Selectivity /% N-LU	Selectivity /% EU	Amine bal. /%	$r_{N\text{-}LU}$[b] /mmol g^{-1} h^{-1}	r_{EU}[c] /mmol g^{-1} h^{-1}
1	393	0	4.8	3.6	0	0[d]	0	0	0	0	0	102	0	0
						2	0	0	0	0	0	100		
						3	0	0	0	0	0	104		
						5	0	0	0	0	0	102		
						7	0	0	0	0	0	102		
						9	0	0	0	0	0	101		
2	393	0.10	4.8	3.7	0.028	0[d]	0.81	12	13	6.5	93	101	0.29	4.2
						2	0.83	10	11	7.2	91	101		
						3	0.57	8.8	10	6.0	92	100		
						5	0.52	7.3	8.0	6.5	91	101		
						7	0.52	6.4	7.0	7.5	91	101		
						9	0.44	5.6	6.4	6.8	88	101		
3	393	0.10	2.4	1.8	0.055	0[d]	2.6	23	23	5.1	96	100	0.46	4.1
						2	1.5	20	21	7.2	93	101		
						3	1.0	18	19	5.1	95	98		
						5	0.90	15	16	5.6	93	100		
						9	1.2	12	13	9.0	89	100		
4	393	0.15	2.4	1.8	0.084	0[d]	1.2	25	26	4.6	95	104	0.14	2.9
						2	1.1	22	23	5.0	95	102		
						3	1.3	22	23	5.6	95	102		
						5	1.3	21	22	5.9	95	102		
						7	1.4	19	20	7.0	93	101		
						9	1.3	16	18	7.2	93	100		
5	393	0.15	1.8	1.4	0.11	0[d]	1.5	40	41	3.8	98	101	0.14	3.5
						2	1.5	35	35	4.3	98	100		
						3	1.6	33	35	4.8	95	101		
						5	1.9	28	30	6.4	94	101		
						7	1.6	25	26	6.3	95	99		
6	393	0.30	2.4	1.8	0.16	0[d]	2.3	66	67	3.4	98	101	0.14	4.0
						2	2.0	57	59	3.5	97	101		
						3	1.9	54	55	3.4	98	101		
						5	2.2	48	51	4.3	94	99		
						7	1.8	43	45	4.1	96	99		
						9	1.4	35	38	3.8	93	100		
7	393	0.30	1.2	0.92	0.33	0[d]	4.9	87	91	5.4	96	103	0.15	2.6
						2	4.6	82	85	5.4	96	102		
						3	5.2	83	88	5.9	94	102		
						5	5.1	79	85	6.1	93	100		
						7	4.8	74	79	6.0	94	101		

8	393	0.50	1.2	0.90	0.56	0[d]	5.6	90	97	5.8	93	101	0.10	1.6
						2	5.3	90	96	5.5	94	101		
						3	5.8	90	97	6.0	93	101		
						5	5.7	90	97	5.9	93	101		
						7	5.5	91	97	5.7	94	100		
						9	5.5	90	96	5.7	94	101		
9	393	1.0	1.2	0.90	1.1	0[d]	5.3	92	97	5.4	95	102	0.047	0.82
						3	5.2	92	96	5.4	95	102		
						5	5.1	93	97	5.2	96	101		
						7	5.4	92	97	5.5	95	102		
						9	5.1	92	96	5.3	96	102		
10	403	0	4.8	3.5	0	0[d]	0	0	0	0	0	104	0	0
						2	0	0	0	0	0	103		
						3	0	0	0	0	0	104		
						5	0	0	0	0	0	104		
						7	0	0	0	0	0	104		
						9	0	0	0	0	0	104		
11	403	0.10	4.8	3.6	0.028	0[d]	1.1	17	18	6.1	92	100	0.41	6.1
						2	1.0	15	16	6.4	92	101		
						3	0.93	13	14	6.6	92	101		
						5	0.81	10	11	7.3	93	100		
						7	0.69	8.7	9.4	7.3	93	102		
						9	0.67	7.9	8.6	7.8	92	102		
12	403	0.10	2.4	1.8	0.057	0[d]	3.3	34	38	8.9	91	99	0.59	6.1
						2	2.5	29	32	7.8	91	100		
						3	2.9	25	28	10	90	99		
						5	2.3	21	23	10	90	99		
						7	2.0	16	18	11	89	100		
						9	1.5	15	17	9.1	89	99		
13	403	0.15	1.8	1.3	0.11	0[d]	6.5	63	70	9.3	90	103	0.58	5.6
						2	5.7	54	60	9.4	89	100		
						3	5.6	50	56	10	89	100		
						5	4.3	39	44	10	88	102		
						7	4.1	36	40	10	90	99		
						9	3.7	30	34	11	87	101		
14	403	0.30	2.4	1.8	0.17	0[d]	6.8	90	97	7.0	93	100	0.41	5.4
						2	5.6	76	82	6.7	93	103		
						3	5.8	71	77	7.5	92	101		
						5	4.6	58	63	7.3	92	102		
						7	3.9	49	53	7.4	92	101		
						9	3.5	43	47	7.3	92	101		
15	403	0.30	1.8	1.3	0.23	0[d]	14	85	>99	14	85	104	0.64	3.8
						3	13	73	87	15	85	103		
						5	13	68	82	15	83	103		
						7	12	60	74	16	82	101		
						9	10	56	67	15	83	102		
16	403	0.50	1.2	0.90	0.55	0[d]	12	87	97	12	90	103	0.21	1.6
						2	12	87	97	12	90	102		
						3	12	87	98	12	89	102		
						7	11	85	97	12	87	100		

						9	12	87	98	12	88	102			
17	403	1.0	1.2	0.87	1.1	0[d]	18	75	97	19	78	102	0.16	0.66	
						3	18	76	97	18	79	101			
						5	20	80	98	20	82	103			
						7	19	78	98	19	80	102			
						9	19	80	98	19	82	102			
18	413	0	4.8	3.6	0	0[d]	0	0	0	0	0	102	0	0	
						2	0	0	0	0	0	102			
						3	0	0	0	0	0	102			
						5	0	0	0	0	0	101			
						7	0	0	0	0	0	102			
						9	0	0	0	0	0	102			
19	413	0.10	4.8	3.7	0.028	0[d]	2.4	22	24	9.9	91	102	0.85	7.7	
						2	2.2	20	22	10	90	102			
						3	1.8	17	18	10	90	102			
						5	1.5	13	15	10	90	101			
						7	1.2	11	12	10	90	102			
						9	1.2	11	12	10	90	101			
20	413	0.15	1.8	1.4	0.11	0[d]	15	82	93	16	85	103	1.3	7.3	
						2	13	70	82	16	86	103			
						3	12	64	76	16	85	103			
						5	11	54	65	16	83	99			
						7	10	46	56	18	83	102			
						9	8.6	43	51	17	84	101			
21	413	0.30	2.4	1.8	0.17	0[d]	14	88	>99	14	86	102	0.84	5.2	
						2	13	80	92	14	86	102			
						3	12	76	87	14	87	102			
						5	11	69	79	14	87	102			
22	413	0.50	1.2	0.90	0.56	0[d]	20	76	98	20	76	100	0.36	1.4	
						2	20	75	98	20	77	101			
						3	20	76	98	21	78	101			
						7	20	76	98	20	78	100			
						9	20	78	97	21	80	101			
23	413	1.0	1.2	0.91	1.1	0[d]	21	76	99	22	76	100	0.19	0.69	
						3	22	75	99	22	77	100			
						5	21	76	98	21	78	101			
						7	22	77	98	22	78	102			
						9	21	75	97	21	77	102			

[a]Reaction conditions: 5.0 mol% (= 8.4 wt%) EDA-CA in EDA solution; CeO_2 with a granule size of 1.0–1.7 mm; 0.9 MPa; fixed-bed flow reactor. Specific conditions are shown in the table.
[b]Formation rate of N-LU.
[c]Formation rate of EU.
[d]The values of conversion, yield, selectivity, and amine balance at TOS = 0 h were calculated by extrapolating the exponentially fitted curve for the data acquired under the steady flow.

Table S23. Effect of reaction temperature on the conversion of EDA-CA in EDA solvent over CeO_2 catalyst in a fixed-bed flow reactor (for the Arrhenius plot in Fig. S22).[a]

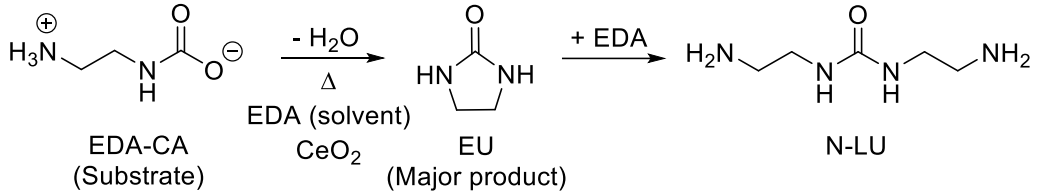

Entry	Temp. /K	W_{cat} /g	F_{sol} /mL h^{-1}	F_{EDA-CA} /mmol h^{-1}	W_{cat}/F_{EDA-CA} /g h $mmol^{-1}$	TOS /h	Yield /% N-LU	Yield /% EU	Conv. /%	Selectivity /% N-LU	Selectivity /% EU	Amine bal. /%	r_{N-LU}[b] /mmol g^{-1} h^{-1}	r_{EU}[c] /mmol g^{-1} h^{-1}	ln(r_{EU} /mmol g^{-1} h^{-1})
1	373	0.15	2.4	1.8	0.083	0[d]	0.40	6.6	7.1	5.7	94	101	0.048	0.79	–0.24
						2	0.39	6.5	6.9	5.7	94	102			
						3	0.41	6.2	6.7	6.2	94	100			
						5	0.33	5.9	6.3	5.3	94	101			
						7	0.35	5.8	6.1	5.8	94	102			
						9	0.37	5.7	6.0	6.2	95	102			
2	383	0.15	2.4	1.8	0.082	0[d]	0.59	13	13	4.5	97	101	0.072	1.5	0.43
						2	0.52	12	12	4.2	96	100			
						3	0.62	12	12	5.0	96	101			
						5	0.48	11	12	4.1	96	102			
						7	0.50	11	11	4.5	96	102			
						9	0.46	10	11	4.3	95	101			
3	393	0.15	2.4	1.8	0.084	0[d]	1.2	25	26	4.6	96	103	0.14	2.9	1.1
						2	1.1	22	23	5.0	95	102			
						3	1.3	22	23	5.6	95	102			
						5	1.3	21	22	5.9	95	102			
						7	1.4	19	20	7.0	93	101			
						9	1.3	16	18	7.2	93	100			
4	403	0.10	4.8	3.6	0.028	0[d]	1.1	17	18	6.1	92	100	0.41	6.1	1.8
						2	1.0	15	16	6.4	92	101			
						3	0.93	13	14	6.6	92	101			
						5	0.81	10	11	7.3	93	100			
						7	0.69	8.7	9.4	7.3	93	102			
						9	0.67	7.9	8.6	7.8	92	102			
5	413	0.10	4.8	3.7	0.028	0[d]	2.4	22	24	10	91	102	0.85	7.7	2.0
						2	2.2	20	22	10	90	102			
						3	1.8	17	18	10	90	102			
						5	1.5	13	15	10	90	101			
						7	1.2	11	12	10	90	102			

[a]Reaction conditions: 5.0 mol% (= 8.4 wt%) EDA-CA in EDA solution; CeO_2 with a granule size of 1.0–1.7 mm; 0.9 MPa; fixed-bed flow reactor. Specific conditions are shown in the table.
[b]Formation rate of N-LU.
[c]Formation rate of EU.
[d]The values of conversion, yield, selectivity, and amine balance at TOS = 0 h were calculated by extrapolating the exponentially fitted curve for the data acquired under the steady flow.

Table S24. Effect of concentration of EDA-CA on the conversion of EDA-CA in EDA solvent over CeO_2 catalyst in a fixed-bed flow reactor (for the determination of reaction order with respect to the concentration of EDA-CA (Fig. S23)).[a]

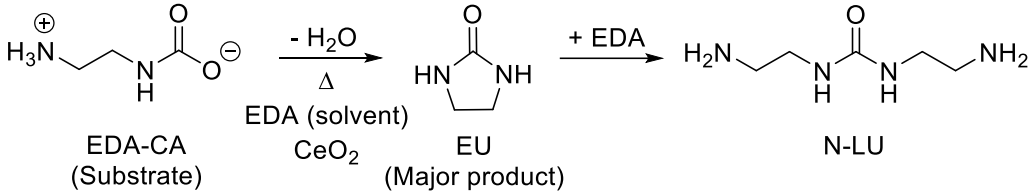

Entry	EDA-CA conc. /M	F_{Sol} /mL h^{-1}	F_{EDA-CA} /mmol h^{-1}	W_{cat}/F_{EDA-CA} /g h $mmol^{-1}$	TOS /h	Yield /%		Conv. /%	Selectivity		Amine bal. /%	r_{EDA-CA}[b] /mmol g^{-1} h^{-1}	ln(r_{EDA-CA} /mmol g^{-1} h^{-1})	ln(EDA-CA conc. /M)
						N-LU	EU		N-LU	EU				
1	0.30	2.4	0.72	0.21	0[c]	2.8	60	59	4.8	96	104	2.8	1.0	–1.2
					2	2.5	51	53	4.7	96	102			
					3	3.1	53	55	5.7	96	104			
					5	2.8	48	51	5.6	95	102			
					7	2.8	45	47	6.0	95	103			
					9	2.7	41	43	6.2	94	100			
2	0.46	2.4	1.1	0.14	0[c]	2.2	41	43	5.2	96	102	3.1	1.1	–0.78
					2	2.0	37	39	5.2	95	102			
					3	2.2	37	39	5.5	95	102			
					5	2.7	36	38	7.1	93	103			
					7	1.9	33	35	5.5	94	101			
					9	2.1	29	31	6.7	93	102			
3	0.75	2.4	1.8	0.084	0[c]	1.2	25	26	4.6	96	103	3.1	1.1	–0.29
					2	1.1	22	23	5.0	95	102			
					3	1.3	22	23	5.6	95	102			
					5	1.3	21	22	5.9	95	102			
					7	1.4	19	20	7.0	93	101			
					9	1.3	16	18	7.2	93	100			
4	1.0	2.4	2.5	0.060	0[c]	1.0	18	19	5.5	95	103	3.1	1.1	0.047
					2	0.94	15	16	5.8	94	103			
					3	1.0	15	16	6.1	95	101			
					5	1.0	13	15	6.8	92	102			
					7	0.83	11	12	6.7	92	101			
					9	0.81	10	11	7.6	92	101			

[a]Reaction conditions: 2.0–7.0 mol% (= 0.30–1.0 M) EDA-CA in EDA solution; CeO_2 with a granule size of 1.0–1.7 mm (W_{cat}) 0.15 g; 393 K; 0.9 MPa; 9 h; fixed-bed flow reactor. Specific conditions are shown in the table.
[b]Conversion rate of EDA-CA.
[c]The values of conversion, yield, selectivity, and amine balance at TOS = 0 h were calculated by extrapolating the exponentially fitted curve for the data acquired under the steady flow.

Table S25. Effect of contact time ($W_{cat}/F_{BA\text{-}CA}$) on the conversion of BA-CA in BA solvent over CeO_2 catalyst at various temperatures in a fixed-bed flow reactor.[a]

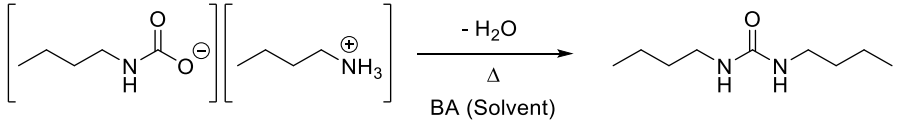

BA-CA (Substrate)

N,*N*'-Dibutylurea (DBU, Target product)

Entry	Temp. /K	W_{cat} /g	F_{Sol} /mL h^{-1}	$F_{BA\text{-}CA}$ /mmol h^{-1}	$W_{cat}/F_{BA\text{-}CA}$ /g h $mmol^{-1}$	TOS /h	Conv.[b] /%	DBU yield[c] /%	DBU sel. /%	Amine bal. /%	r_{DBU}[d] /mmol g^{-1} h^{-1}
1	393	1.0	1.2	0.50	2.0	0[e]	5.9	6.0	>99	102	0.030
						7	6.0	6.0	99	102	
						8	6.1	6.1	>99	102	
						9	5.7	5.7	>99	101	
2	393	1.5	0.60	0.27	5.6	0[e]	26	26	>99	101	0.047
						7	27	27	99	104	
						8	26	26	>99	100	
						9	26	26	>99	100	
3	393	2.0	0.60	0.25	7.9	0[e]	32	33	>99	103	0.042
						8	34	34	>99	101	
						9	32	33	>99	103	
						10	31	31	>99	105	
4	403	0.70	2.4	1.2	0.60	0[e]	6.0	5.9	99	99	0.10
						5	6.1	6.0	98	99	
						7	6.3	6.4	>99	99	
						9	5.6	5.5	99	99	
5	403	1.0	1.2	0.58	1.7	0[e]	13	13	97	98	0.074
						7	13	12	97	99	
						8	13	12	96	97	
						9	14	13	97	98	
6	403	1.0	0.60	0.27	3.7	0[e]	29	28	99	98	0.076
						7	28	28	99	98	
						8	29	28	98	97	
						9	29	29	99	98	
7	403	1.5	0.6	0.27	5.6	0[e]	50	51	>99	100	0.091
						7	53	54	>99	100	
						8	51	52	>99	101	
						9	45	46	>99	99	
8	403	2.0	0.60	0.27	7.3	0[e]	64	64	>99	102	0.088
						8	66	65	97	102	
						9	64	64	>99	103	
						10	63	63	>99	101	
9	413	0.70	2.4	1.2	0.59	0[e]	16	16	>99	98	0.27
						5	16	17	>99	100	
						7	16	16	98	98	
						9	15	16	>99	98	
10	413	1.0	1.2	0.58	1.7	0[e]	38	38	99	99	0.22
						5	38	38	99	98	
						7	37	38	>99	100	
						9	38	37	98	98	

11	413	1.0	0.60	0.27	3.7	0[e]	75	76	>99	98	0.21
						7	75	75	>99	99	
						8	78	79	>99	98	
						9	72	74	>99	97	

[a]Reaction conditions: 5.0 mol% (= 7.7 wt%) BA-CA in BA solution; CeO_2 with a granule size of 1.0–1.7 mm; 0.9 MPa; fixed-bed flow reactor. Specific conditions are shown in the table.
[b]Determined by ^{1}H NMR.
[c]Quantified by GC.
[d]Formation rate of *N*,*N*'-dibutylurea.
[e]The values of yield, conversion, selectivity, and amine balance at TOS = 0 h were calculated by averaging the data acquired under the steady flow.

Table S26. Effect of reaction temperature on the conversion of BA-CA in BA solvent over CeO_2 catalyst at various temperatures in a fixed-bed flow reactor. (for the Arrhenius plot in Fig. S25).[a]

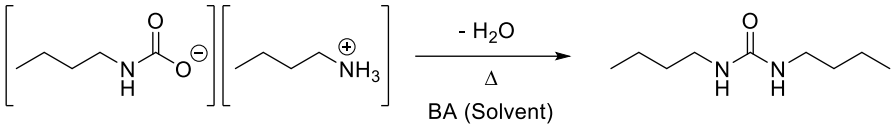

BA-CA (Substrate) → *N*,*N*'-Dibutylurea (DBU, Target product)

Entry	Temp. /K	W_{cat} /g	F_{Sol} /mL h^{-1}	$F_{BA\text{-}CA}$ /mmol h^{-1}	$W_{cat}/F_{BA\text{-}CA}$ /g h mmol^{-1}	TOS /h	Conv.[b] /%	DBU yield[c] /%	DBU sel. /%	Amine bal. /%	r_{DBU}[d] /mmol g^{-1} h^{-1}	ln(r_{DBU} /mmol g^{-1} h^{-1})
1	393	2.0	0.60	0.25	7.9	0[e]	32	33	>99	103	0.042	–3.2
						8	34	34	>99	101		
						9	32	33	>99	103		
						10	31	31	>99	105		
2	403	0.70	2.4	1.2	0.59	0[e]	6.0	5.9	99	99	0.10	–2.3
						5	6.1	6.0	98	99		
						7	6.3	6.4	>99	99		
						9	5.6	5.5	98	99		
3	413	0.70	2.4	1.2	0.59	0[e]	16	16	>99	98	0.27	–1.3
						5	16	17	>99	100		
						7	16	16	98	98		
						9	15	16	>99	98		

[a]Reaction conditions: 5.0 mol% (= 7.7 wt%) BA-CA in BA solution; CeO_2 with a granule size of 1.0–1.7 mm; 0.9 MPa; fixed-bed flow reactor. Specific conditions are shown in the table.
[b]Determined by ^{1}H NMR.
[c]Quantified by GC.
[d]Formation rate of *N*,*N*'-dibutylurea.
[e]The values of yield, conversion, selectivity, and amine balance at TOS = 0 h were calculated by averaging the data acquired under the steady flow.

Table S27. Conversions of various organic carbamates in amine solvents without CeO_2 catalyst under mild conditions in a batch reactor.[a]

Entry	Substrate	Amine solvent	Detected compounds /mmol					Amine bal. /%
			Substrate (used as a substrate)	Urea derivative	Alkylcarbamic salt	Amine (used as a solvent)	Others	
1[b]	 2CC	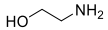 2AOL	0	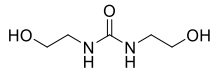 0.94	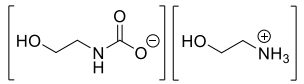 0.09	100	0	99
2[b]	 3CC	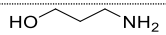 3AOL	0	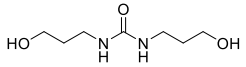 0.97	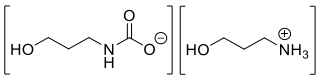 0.12	99	0	101
3[c]	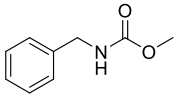 Methyl *N*-benzylcarbamte	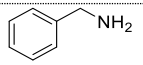 Benzylamine	0.95	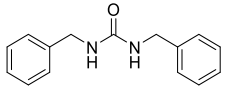 <0.01	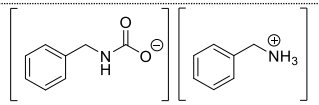 _d	95	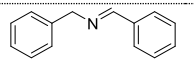 0.17[e]	94
4[c]		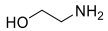 2AOL	0.92	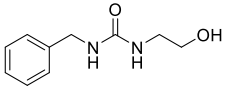 0	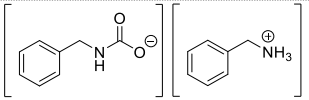 _d	103	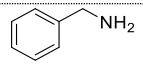 0.10	103
5[c]	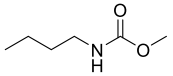 Methyl *N*-butylcarbamate	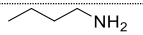 *n*-Butylamine	1.1	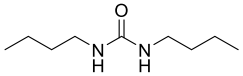 <0.01	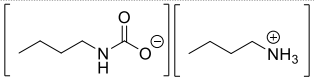 _d	93	0	93
6[c]		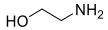 2AOL	0.97	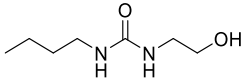 0	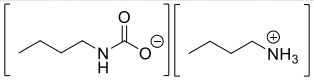 _d	104	0	106

[a]Reaction conditions: substrate 1.0 mmol; amine solvent 100 mmol; Ar 1.0 MPa (at r.t.); 373 K; 1 h; batch reactor (autoclave).
[b]Each compound was quantified by ^{1}H NMR.
[c]Each compound was quantified by GC-FID.
[d]BZA-CA and BA-CA were quantified as BZA and BA, respectively, by GC-FID due to the thermal degradation of each alkylcarbamic salt.
[e]Generated in the vaporization chamber of GC-FID.[S11]

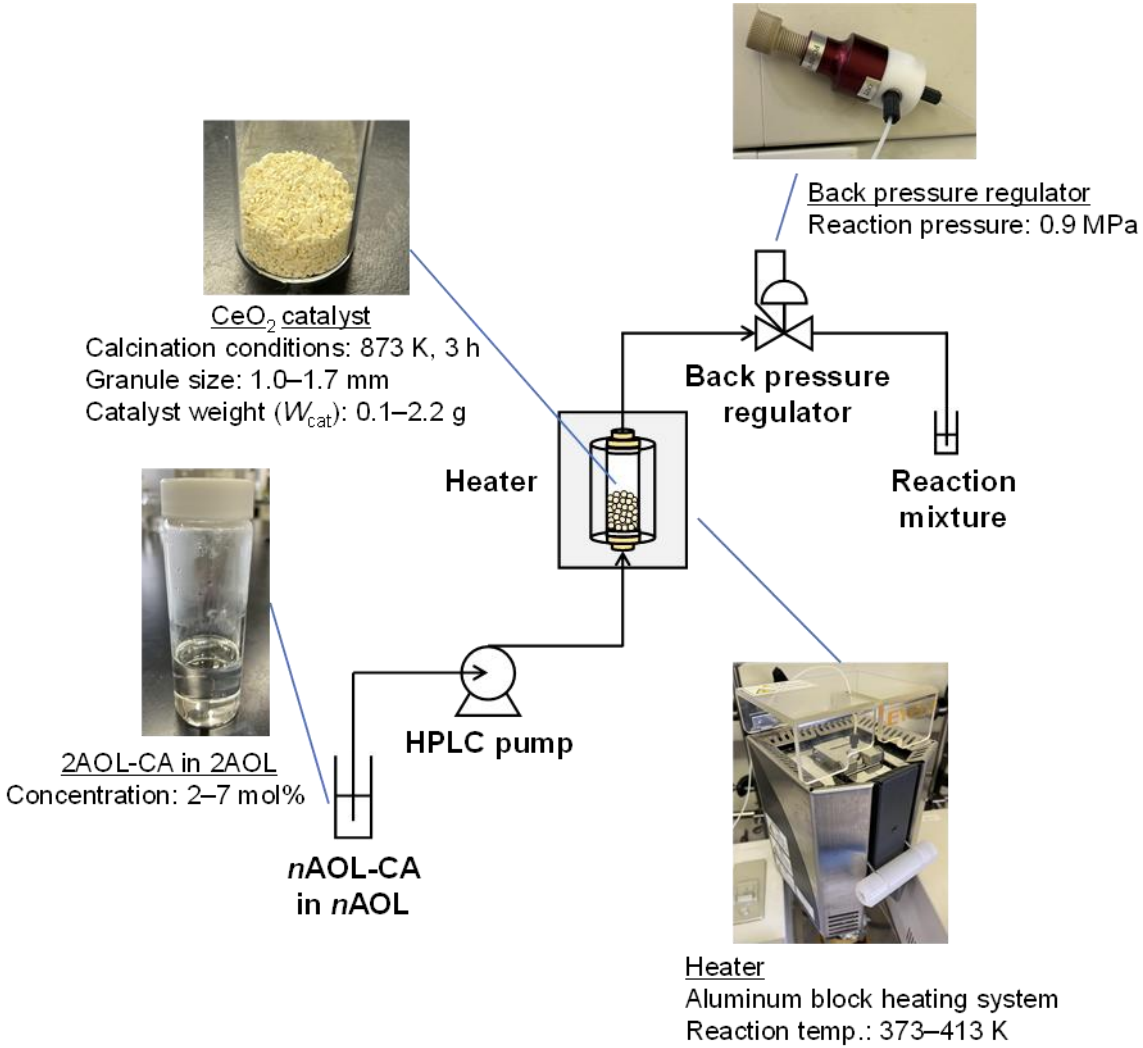

Fig. S1 Schematic diagram of fixed-bed flow reactor used in this study.

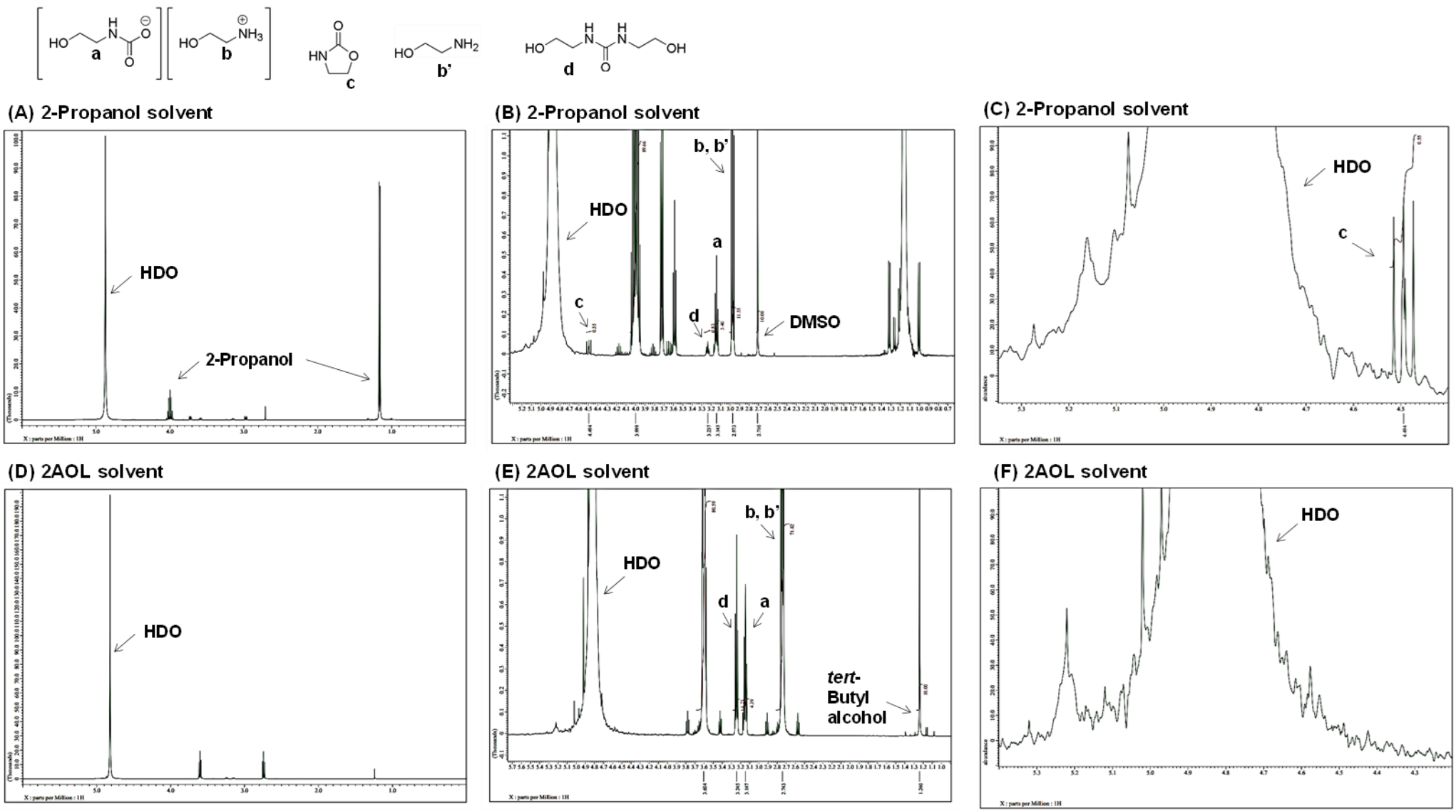

Fig. S2 Typical ^{1}H NMR spectra of reaction mixtures after the conversion of 2AOL-CA in (A–C) 2-propanol solvent and (D–F) 2AOL solvent, acquired in D_2O in the presence of either DMSO or *tert*-butyl alcohol as an internal standard. The panels B+C and E+F are the expanded versions of A and D, respectively.
Reaction conditions for panels A–C: 2AOL-CA 10 mmol; CeO_2 1.0 mmol; 2-propanol 200 mmol; Ar 1.0 MPa (at r.t.); 393 K; 1 h; batch reactor (autoclave).
Reaction conditions for panels D–F: 2AOL-CA 10 mmol; CeO_2 1.0 mmol; 2AOL 100 mmol; Ar 1.0 MPa (at r.t.); 393 K; 1 h; batch reactor (autoclave).

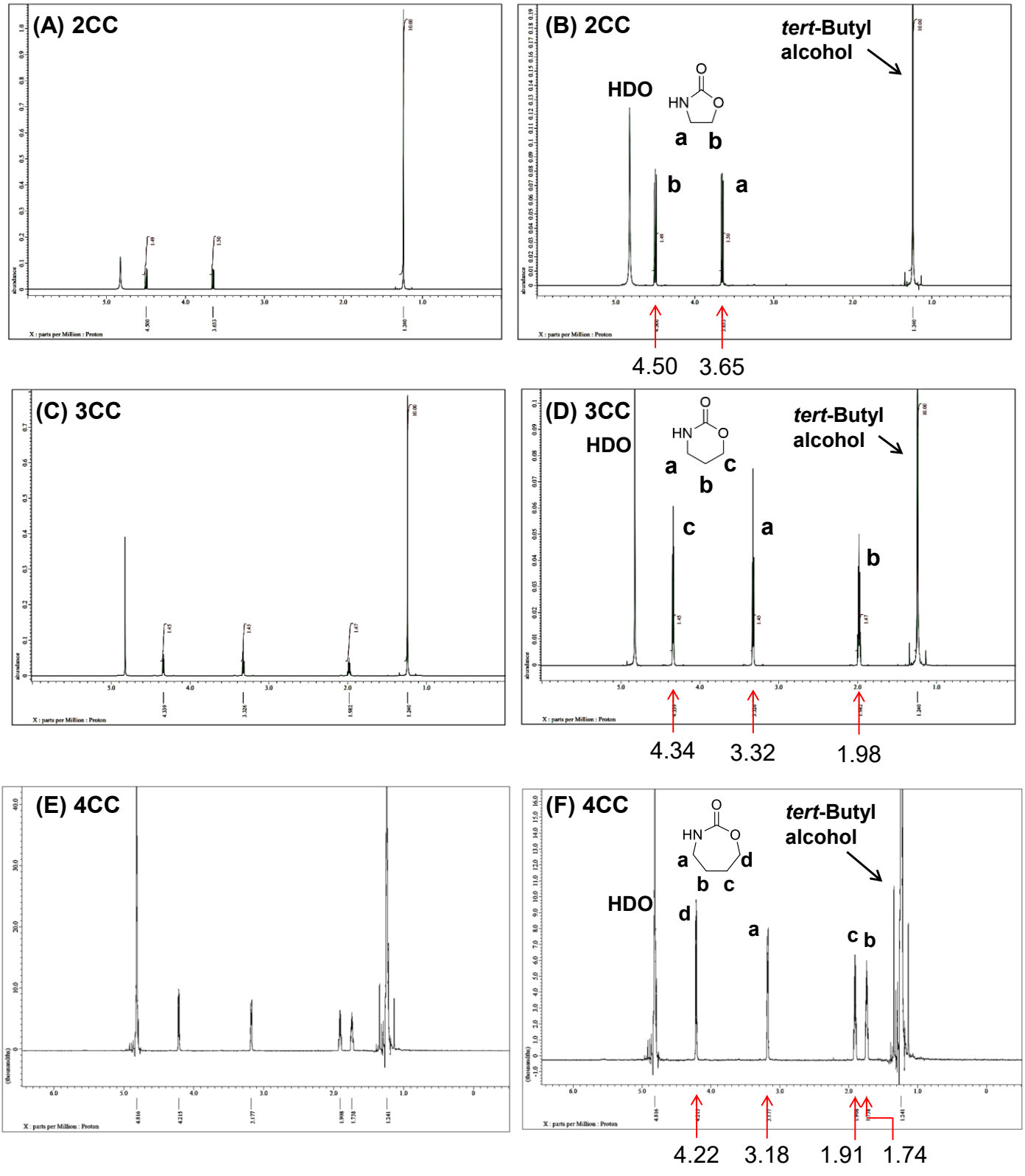

Fig. S3 ^{1}H NMR spectra of cyclic carbamates purchased from chemical companies, acquired in D_2O in the presence of *tert*-butyl alcohol as an internal standard: (A, B) 2CC; (C, D) 3CC; (E, F) 4CC.
The panels B, D, and F are the expanded versions of A, C, and E, respectively.

2CC: ^{1}H NMR (400 MHz, D_2O): δ 4.50 (2H, t, J = 8.2 Hz); 3.65 (2H, t, J = 8.2 Hz).
3CC: ^{1}H NMR (600 MHz, D_2O): δ 4.34 (2H, t, J = 5.2 Hz); 3.32 (2H, t, J = 6.0 Hz); 1.98 (2H, m).
4CC: ^{1}H NMR (600 MHz, D_2O): δ 4.22 (2H, t, J = 5.4 Hz); 3.18 (2H, t, J = 5.4 Hz); 1.91 (2H, m); 1.74 (2H, m).

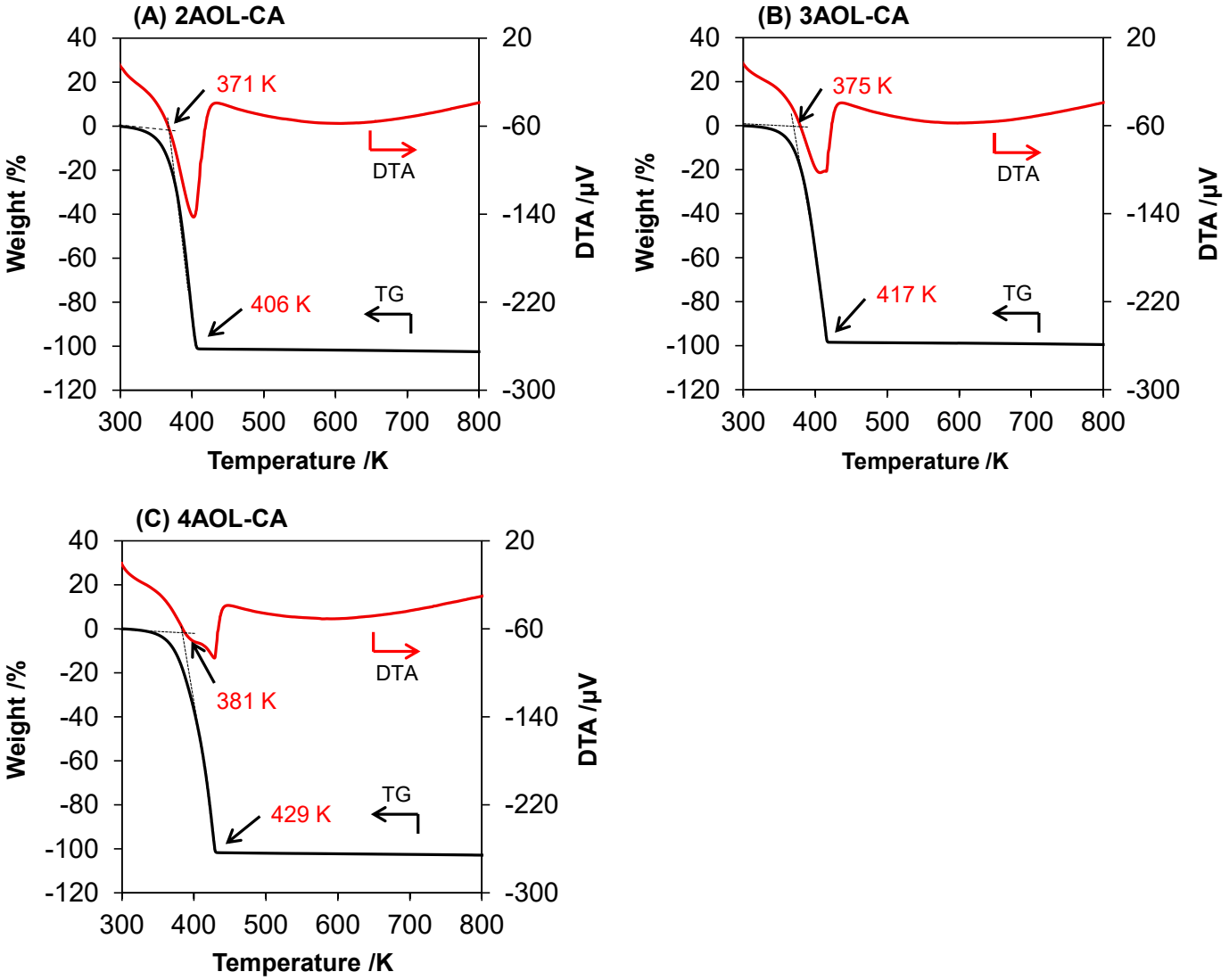

Fig. S4 TG-DTA profiles for *n*AOL-CA in a N_2 flow.
Analysis conditions: *n*AOL-CA 10–12 mg; N_2 flow 30 mL min^{-1}; ramp rate 10 K min^{-1}; 300–800 K.
The temperatures where *n*AOL-CA began to decompose were decomposed (371, 375, and 381 K, respectively) were determined from the intersection point of two tangent lines (dotted lines in the figure).

Solute	2AOL-CA	3AOL-CA	4AOL-CA	EDA-CA	BA-CA
Solvent	2AOL	3AOL	4AOL	EDA	BA

Fig. S5 Picture of the amine solutions containing 5.0 mol% of corresponding alkylcarbamic salt.

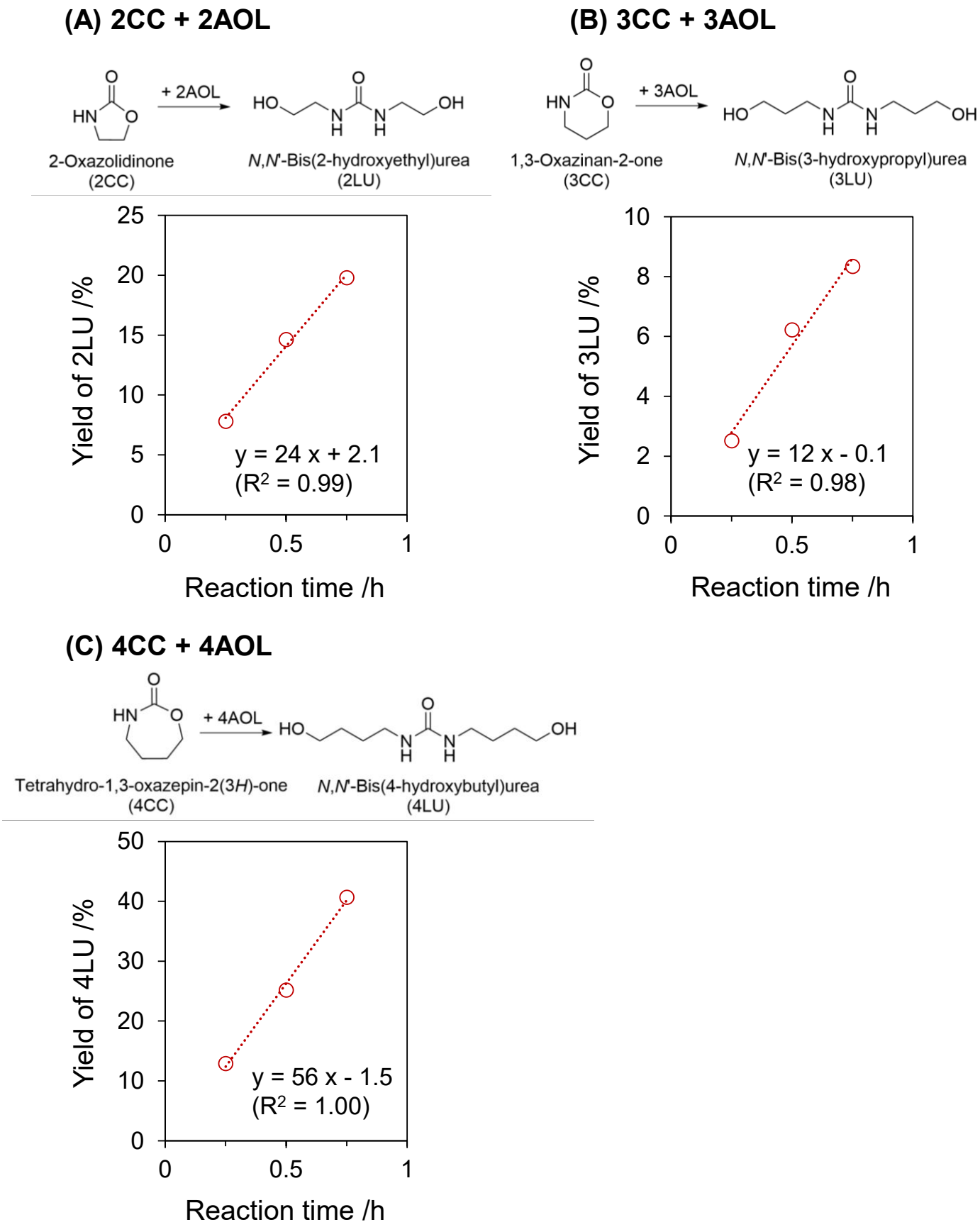

Fig. S6 Conversion of *n*CC in corresponding *n*AOL solvent at 333 K in a batch reactor (pressure-resistant glass tube). Reaction conditions for panel A and B: *n*CC 1.0 mmol; *n*AOL 50 mmol; air 0.1 MPa; 333 K; batch reactor (pressure-resistant glass tube).
Reaction conditions for panel C: 4CC 0.1 mmol; 4AOL 50 mmol; air 0.1 MPa; 333 K; batch reactor (pressure-resistant glass tube). The reactions were continuously operated, and the sampling of 0.3 g of reaction mixture was conducted at each reaction time shown in the table. The reaction results were estimated on the basis of the initial reaction solution.
The detailed data are shown in Table S7.

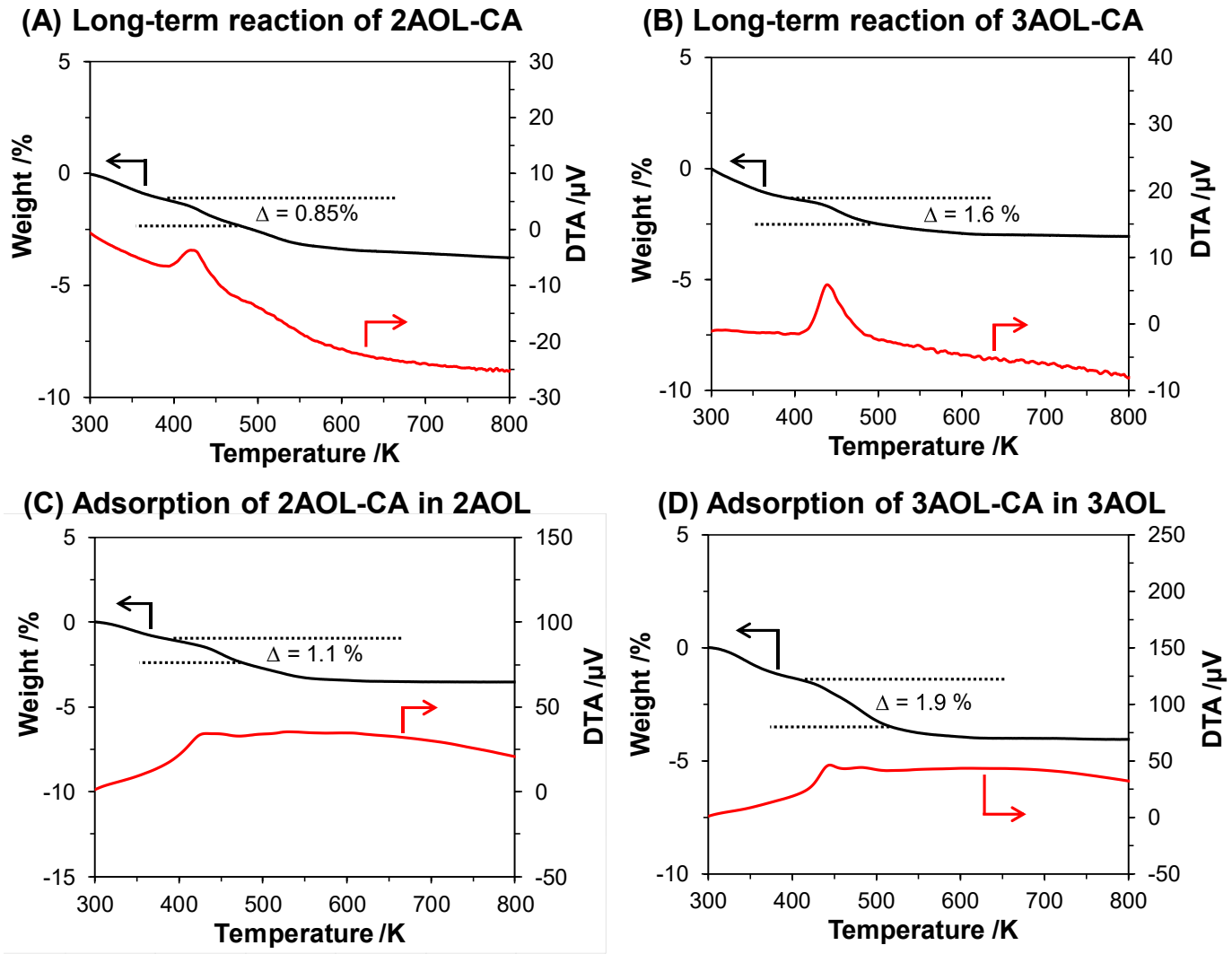

Fig. S7 (A, B) TG-DTA profiles for the spent CeO_2 after the long-term operation of *n*AOL-CA in *n*AOL. (C, D) TG-DTA profiles for CeO_2 soaked into *n*AOL-CA in *n*AOL.
Analysis conditions: sample *ca.* 10 mg; air flow 30 mL min^{-1}; ramp rate 10 K min^{-1}; 300–800 K.
Reaction conditions for the conversion of 2AOL-CA (panel A): 5.0 mol% (= 8.2 wt%) 2AOL-CA in 2AOL solution; CeO_2 with a granule size of 1.0–1.7 mm (W_{cat}) 1.0 g; F_{sol} = 1.7 mL h^{-1} ($F_{2AOL\text{-}CA}$ = 1.4 mmol h^{-1}); $W_{cat}/F_{2AOL\text{-}CA}$ = 0.71 g h $mmol^{-1}$; 413 K; 0.9 MPa; TOS 57 h; fixed-bed flow reactor.
Reaction conditions for the conversion of 3AOL-CA (panel B): 5.0 mol% (= 7.7 wt%) 3AOL-CA in 3AOL solution; CeO_2 with a granule size of 1.0–1.7 mm (W_{cat}) 1.0 g; F_{sol} = 0.60 mL h^{-1} ($F_{3AOL\text{-}CA}$ = 0.25 mmol h^{-1}); $W_{cat}/F_{3AOL\text{-}CA}$ = 4.0 g h $mmol^{-1}$; 413 K; 0.9 MPa; TOS 194 h; fixed-bed flow reactor.
Adsorption conditions of 2AOL-CA (panel C): CeO_2 (powder form) 1.0 g; 2AOL-CA 2.0 g; 2AOL 22 g; room temperature; 1 h.
Adsorption conditions of 3AOL-CA (panel D): CeO_2 (powder form) 1.0 g; 3AOL-CA 2.0 g; 2AOL 24 g; room temperature; 1 h.

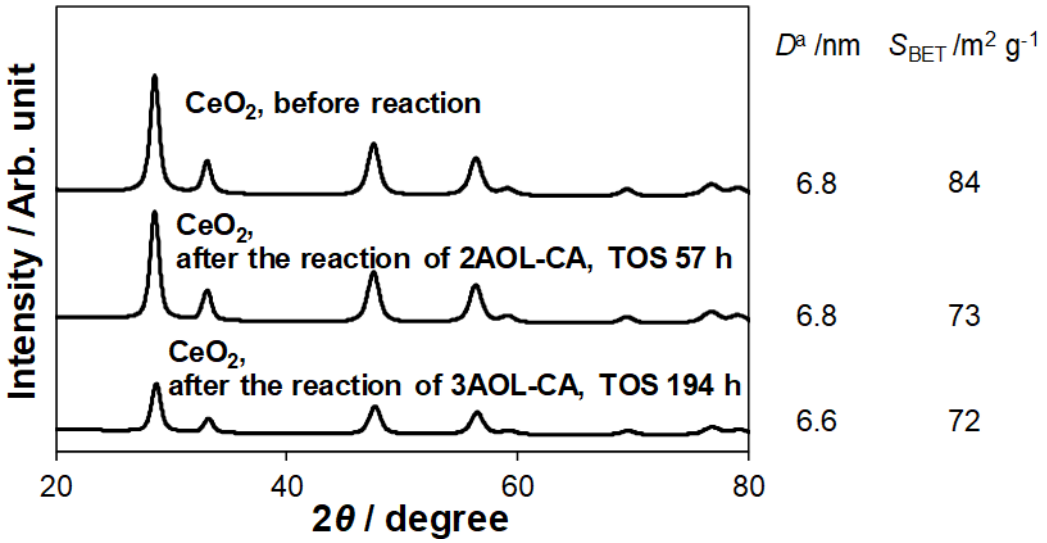

Fig. S8 XRD patterns of the spent CeO_2 catalysts before/after the long-term operation of the conversion of *n*AOL-CA in corresponding *n*AOL solvent in a fixed-bed flow reactor.
[a]The crystallite size (*D*) in the figure was calculated using the diffraction peak at 48° and the Scherrer equation.
Reaction conditions for the conversion of 2AOL-CA: 5.0 mol% (= 8.2 wt%) 2AOL-CA in 2AOL solution; CeO_2 with a granule size of 1.0–1.7 mm (W_{cat}) 1.0 g; F_{sol} = 1.7 mL h^{-1} ($F_{2AOL\text{-}CA}$ = 1.4 mmol h^{-1}); $W_{cat}/F_{2AOL\text{-}CA}$ = 0.7 g h $mmol^{-1}$; 413 K; 0.9 MPa; TOS 57 h; fixed-bed flow reactor.
Reaction conditions for the conversion of 3AOL-CA: 5.0 mol% (= 7.7 wt%) 3AOL-CA in 3AOL solution; CeO_2 with a granule size of 1.0–1.7 mm (W_{cat}) 1.0 g; F_{sol} = 0.60 mL h^{-1} ($F_{3AOL\text{-}CA}$ = 0.25 mmol h^{-1}); $W_{cat}/F_{3AOL\text{-}CA}$ = 4.0 g h $mmol^{-1}$; 413 K; 0.9 MPa; TOS 194 h; fixed-bed flow reactor.

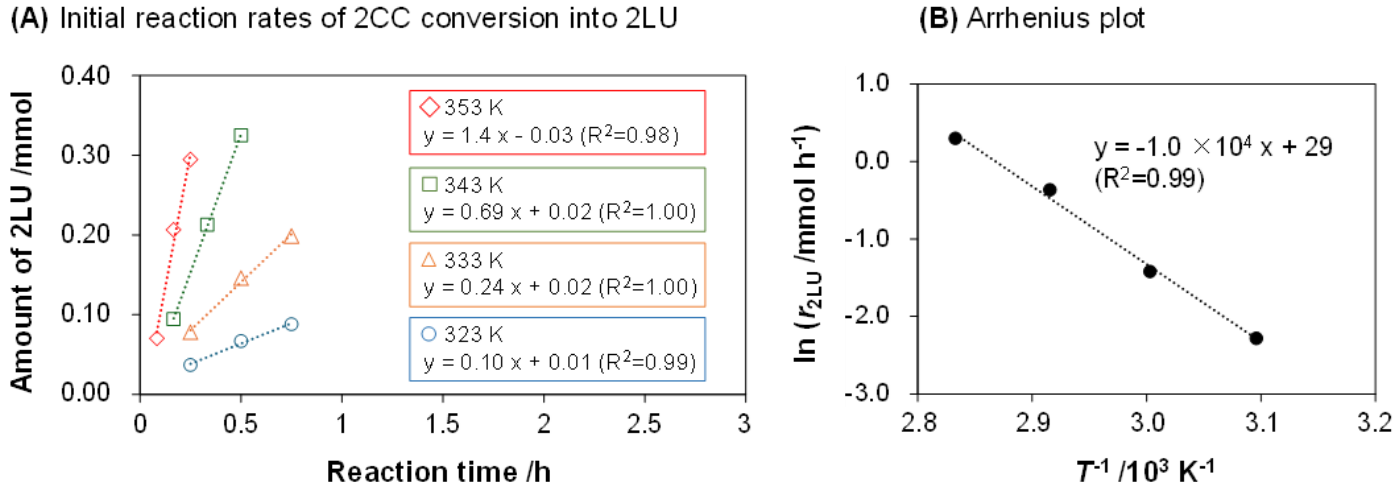

Fig. S9 (A) Initial formation rates of 2LU (r_{2LU}) from 2CC and 2AOL without CeO_2 catalyst at various temperatures and (B) Arrhenius plot based on r_{2LU}.
Reaction conditions: 2CC 1.0 mmol; 2AOL 50 mmol; air 1 atm; 323–353 K; batch reactor (pressure-resistant glass tube).
The detailed data are shown in Table S10.

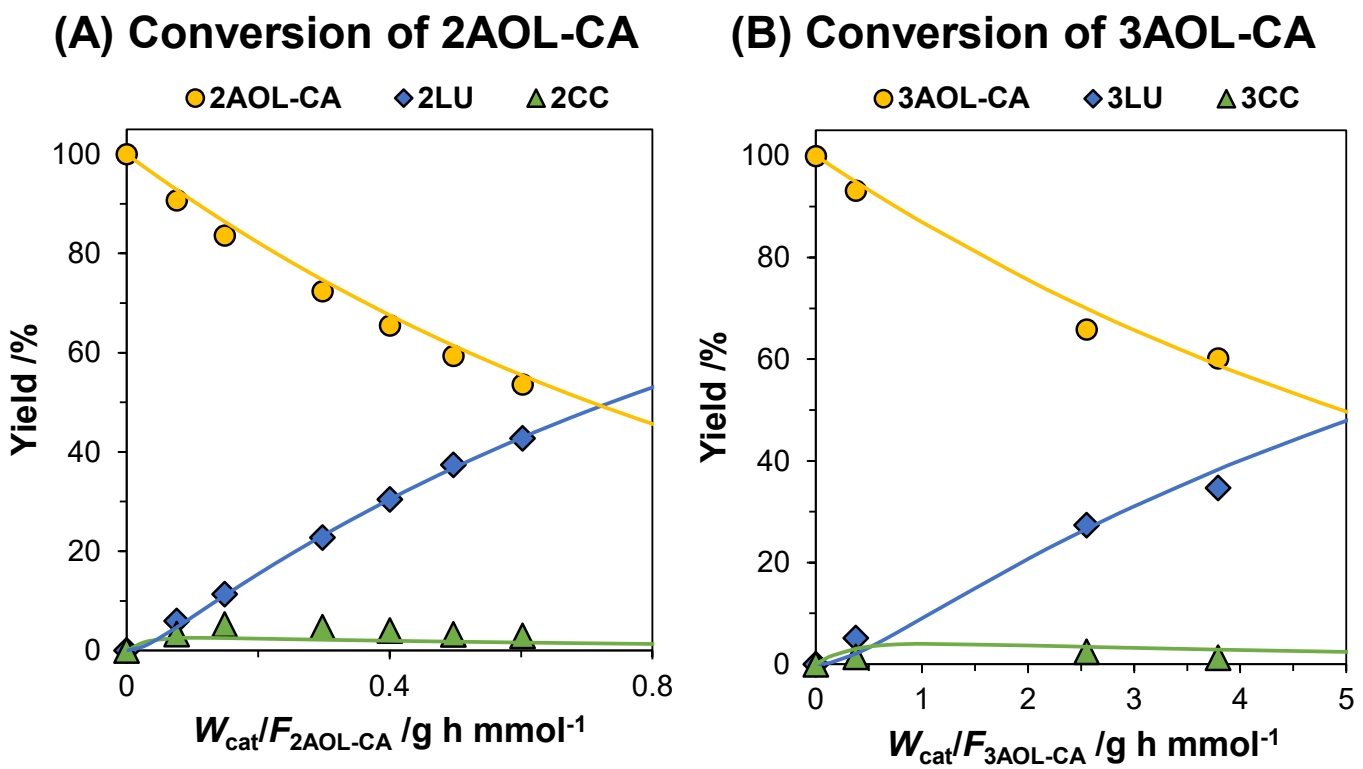

Fig. S10 Kinetic fitting analyses for the conversion of 2AOL-CA and 3AOL-CA over CeO_2 catalyst at 393 K. The dots are the raw experimental data (from Tables S6 and S13), and the lines are the fitting curves based on the kinetic simulations.
Simulation conditions for panel A: 5.0 mol% (= 8.2 wt%) 2AOL-CA in 2AOL solution.
Reaction conditions for panel A: 5.0 mol% (= 8.2 wt%) 2AOL-CA in 2AOL solution; CeO_2 with a granule size of 1.0–1.7 mm (W_{cat}) 0–0.60 g; F_{sol} = 1.2–2.4 mL h^{-1} ($F_{2AOL-CA}$ = 1.0–2.0 mmol h^{-1}); $W_{cat}/F_{2AOL-CA}$ = 0–0.60 g h mmol^{-1}; 393 K; 0.9 MPa; 9 h.
Simulation conditions for panel B: 5.0 mol% (= 7.7 wt%) 3AOL-CA in 3AOL solution.
Reaction conditions for panel B: 5.0 mol% (= 7.7 wt%) 3AOL-CA in 3AOL solution; CeO_2 with a granule size of 1.0–1.7 mm (W_{cat}) 0–1.5 g; F_{sol} = 0.60–2.4 mL h^{-1} ($F_{3AOL-CA}$ = 0–1.6 mmol h^{-1}); $W_{cat}/F_{3AOL-CA}$ = 0–3.8 g h mmol^{-1}; 393 K; 0.9 MPa; TOS 9 h; fixed-bed flow reactor.

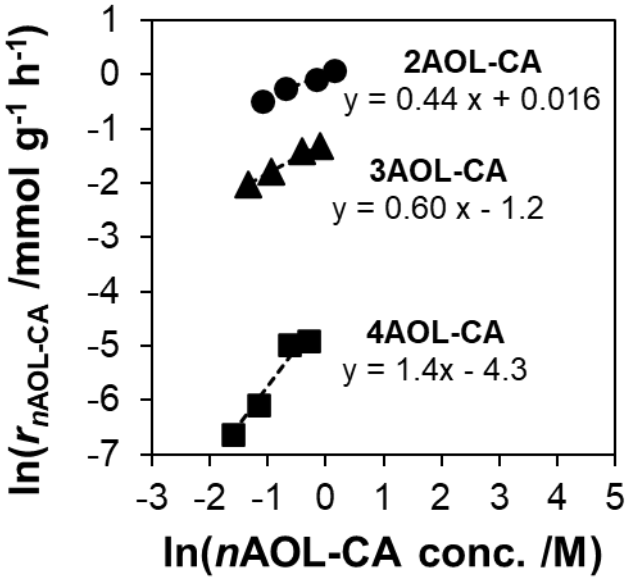

Fig. S11 Double logarithmic plots of the initial conversion rates of *n*AOL-CA as a function of the concentration of *n*AOL-CA in corresponding *n*AOL solvent.
Reaction conditions for the conversion of 2AOL-CA: 2.0–7.0 mol% (= 0.34–1.2 M) 2AOL-CA in 2AOL solution; CeO_2 with a granule size of 1.0–1.7 mm (W_{cat}) 0.30 g; F_{sol} = 1.2 mL h^{-1} ($F_{2AOL\text{-}CA}$ = 0.40–1.4 mmol h^{-1}); $W_{cat}/F_{2AOL\text{-}CA}$ = 0.22–0.75 g h $mmol^{-1}$; 393 K; 0.9 MPa; TOS 9 h; fixed-bed flow reactor.
Reaction conditions for the conversion of 3AOL-CA: 2.0–7.0 mol% (= 0.26–0.91 M) 3AOL-CA in 3AOL solution; CeO_2 with a granule size of 1.0–1.7 mm (W_{cat}) 1.0 g; F_{sol} = 1.2 mL h^{-1} ($F_{3AOL\text{-}CA}$ = 0.32–1.1 mmol h^{-1}); $W_{cat}/F_{3AOL\text{-}CA}$ = 0.91–3.2 g h $mmol^{-1}$; 393 K; 0.9 MPa; TOS 9 h; fixed-bed flow reactor.
Reaction conditions for the conversion of 4AOL-CA: 2.0–7.0 mol% (= 0.20–0.73 M) 4AOL-CA in 4AOL solution; CeO_2 with a granule size of 1.0–1.7 mm (W_{cat}) 2.2 g; F_{sol} = 0.12 mL h^{-1} ($F_{4AOL\text{-}CA}$ = 0.024–0.088 mmol h^{-1}); $W_{cat}/F_{4AOL\text{-}CA}$ = 25–92 g h $mmol^{-1}$; 393 K; 0.9 MPa; TOS 40–100 h; fixed-bed flow reactor.
The detailed data are shown in Tables S12, S16, and S21.

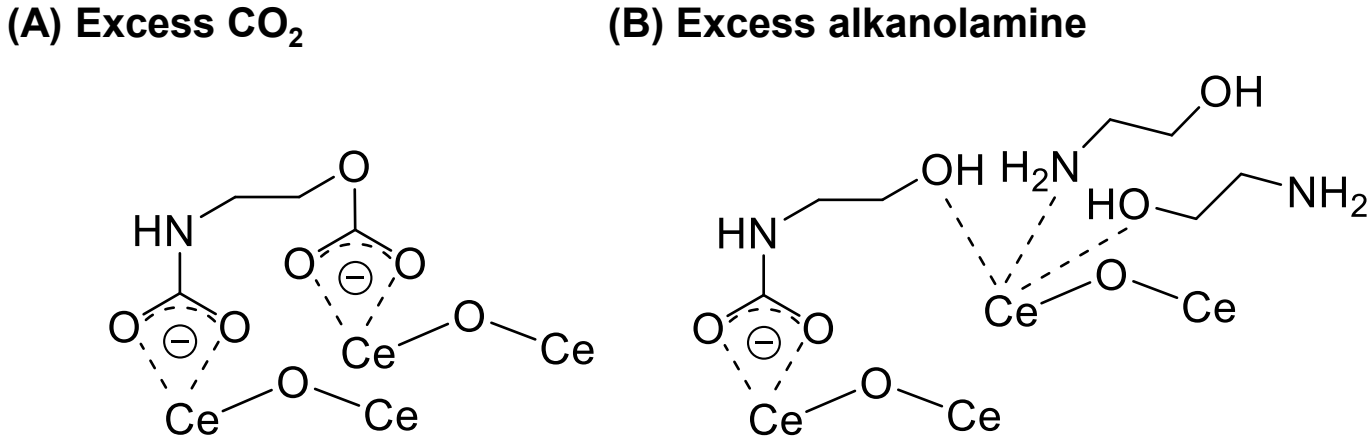

Fig. S12 Plausible adsorption states of substrates on the surface of CeO_2 catalyst in two different reaction systems: (A) the reaction of 2AOL with high-pressure CO_2 (*i.e.*, excess amount of CO_2 against 2AOL) and (B) the conversion of 2AOL-CA in 2AOL solvent.

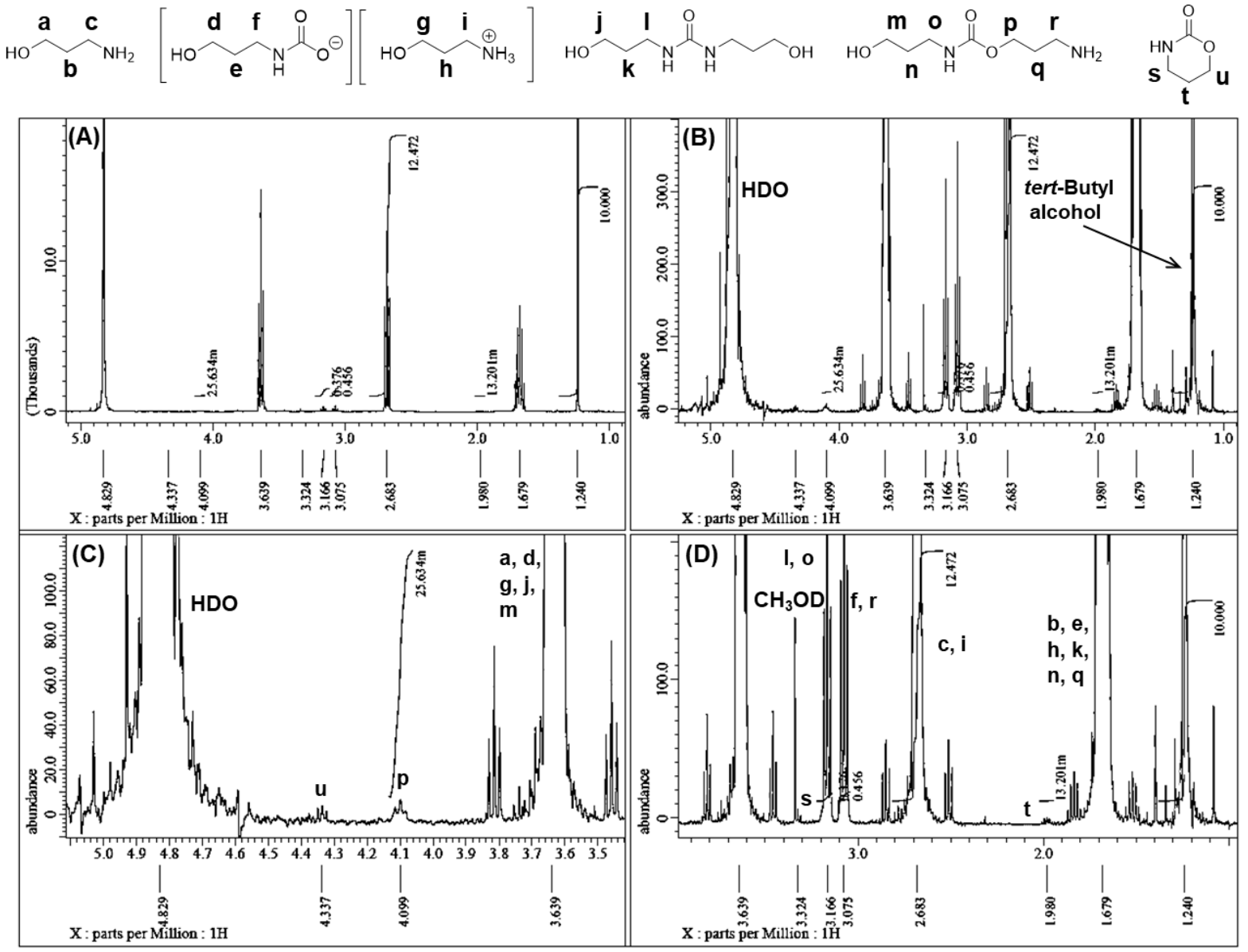

Fig. S13 (A) Typical ^{1}H NMR spectrum of the reaction mixture after the conversion of 3AOL-CA in a fixed-bed flow reactor, acquired in D_2O in the presence of *tert*-butyl alcohol as an internal standard. (B–D) Expanded version of panel A.
Reaction conditions: 5.0 mol% (= 7.7 wt%) 3AOL-CA in 3AOL solution; CeO_2 with a granule size of 1.0–1.7 mm; (W_{cat}) 1.0 g; F_{sol} = 0.60 mL h^{-1} ($F_{3AOL\text{-}CA}$ = 0.41 mmol h^{-1}); $W_{cat}/F_{3AOL\text{-}CA}$ = 2.5 g h $mmol^{-1}$; 393 K; 0.9 MPa; TOS 9 h; fixed-bed flow reactor.

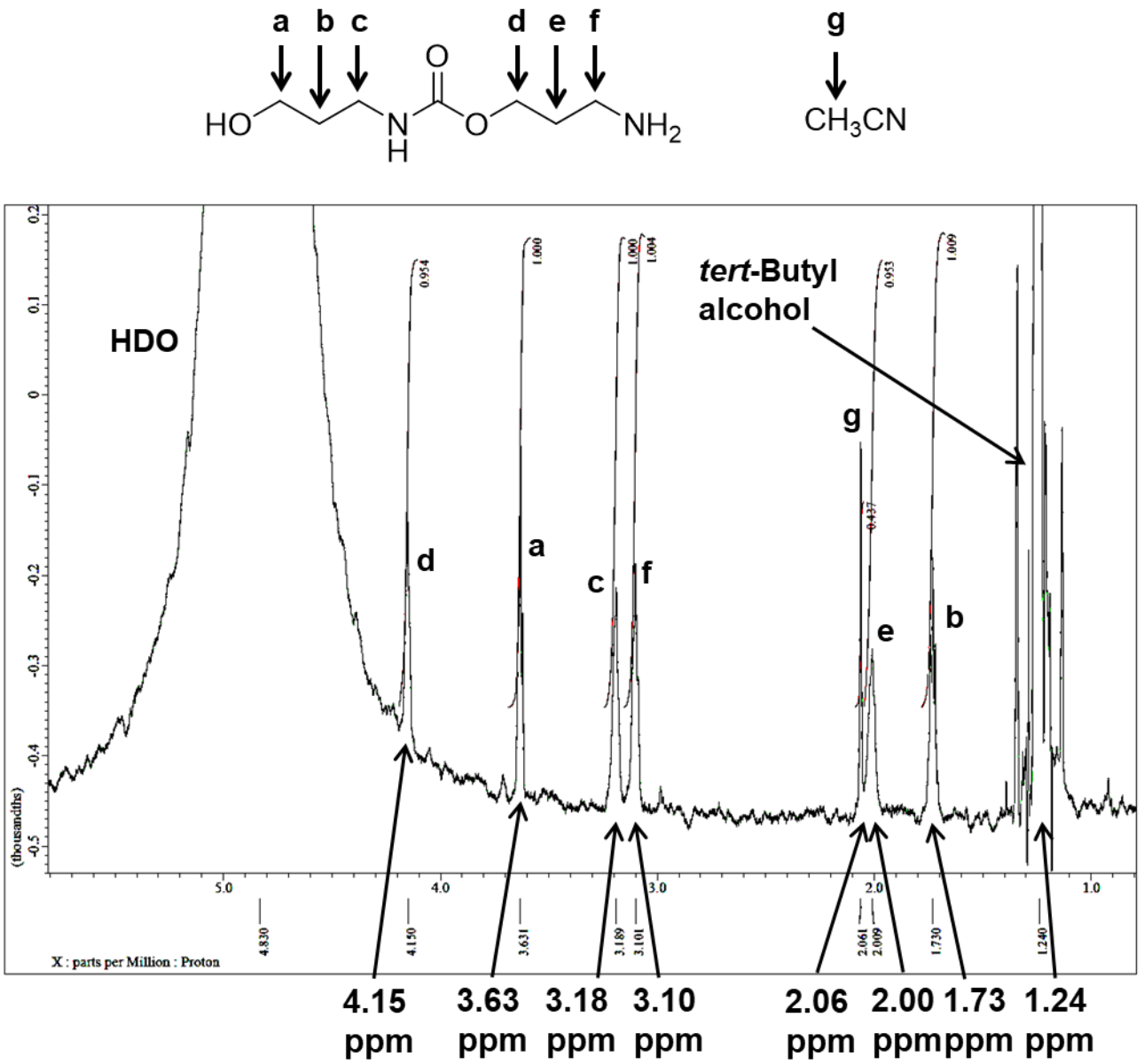

Fig. S14 ^{1}H NMR spectrum of 3LC isolated from the reaction mixture after the conversion of 3AOL-CA in 3AOL solvent over CeO_2 catalyst in a fixed-bed flow reactor, acquired in D_2O in the presence of *tert*-butyl alcohol as an internal standard.
Acetonitrile detected in this spectrum (*i.e.*, singlet signal "g") was derived from the mobile phase of HPLC used for the isolation of 3LC from the reaction mixture.
Reaction conditions: 5.0 mol% (= 7.7 wt%) 3AOL-CA in 3AOL solution; CeO_2 with a granule size of 1.0–1.7 mm (W_{cat}) 1.0 g; F_{sol} = 0.60 mL h^{-1} ($F_{3AOL\text{-}CA}$ = 0.41 mmol h^{-1}); $W_{cat}/F_{3AOL\text{-}CA}$ = 2.5 g h mmol^{-1}; 393 K; 0.9 MPa; TOS 9 h; fixed-bed flow reactor.

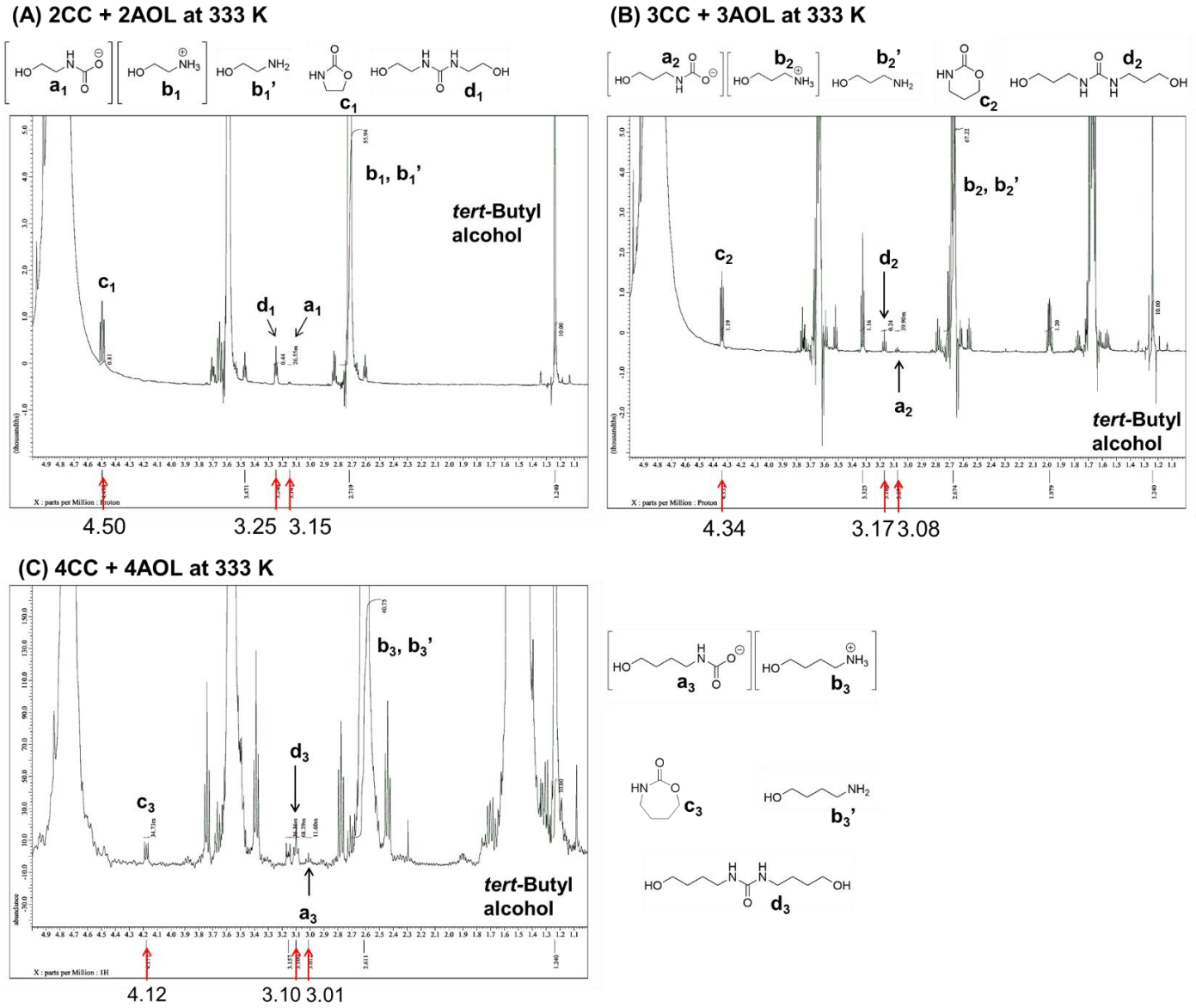

Fig. S15 ^{1}H NMR spectra of reaction mixtures after the conversion of *n*CC in corresponding *n*AOL solvent at 333 K in a batch reactor (pressure-resistant glass tube).
Reaction conditions for panels A and B: *n*CC 1.0 mmol; *n*AOL 50 mmol; air 0.1 MPa; 333 K; 45 min; batch reactor (pressure-resistant glass tube).
Reaction conditions for panel C: 4CC 0.1 mmol; 4AOL 50 mmol; air 0.1 MPa; 333 K; 45 min; batch reactor (pressure-resistant glass tube). These reactions were continuously operated, and the sampling of 0.3 g of reaction mixture was conducted at each reaction time shown in the table.
The detailed data are shown in Table S7.

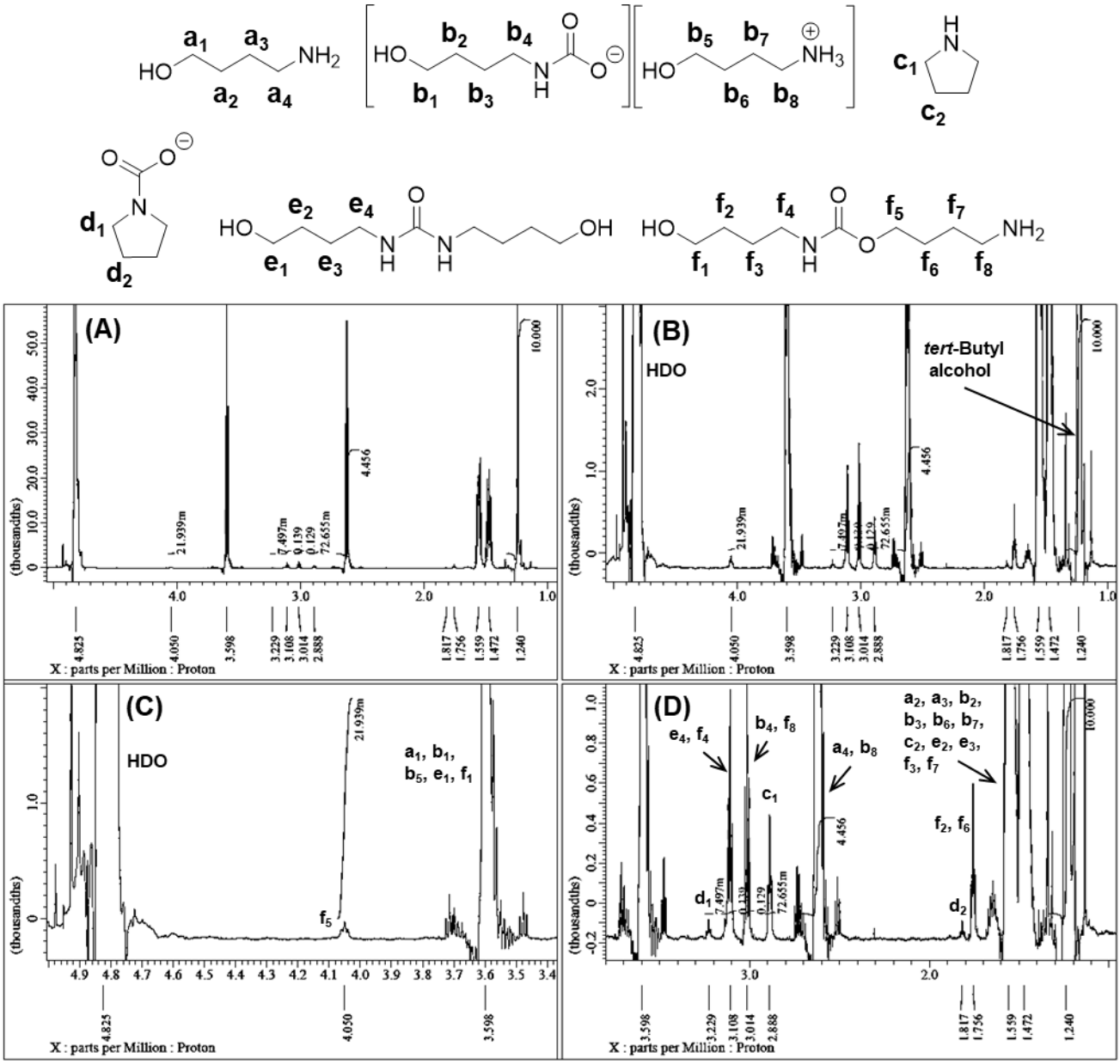

Fig. S16 (A) Typical ^{1}H NMR spectrum of reaction mixtures after the conversion of 4AOL-CA in a fixed-bed flow reactor, acquired in D_2O in the presence of *tert*-butyl alcohol as an internal standard. (B–D) Expanded spectrum of panel A. Reaction conditions: 5.0 mol% (= 7.2 wt%) 4AOL-CA in 4AOL solution; CeO_2 with a granule size of 1.0–1.7 mm (W_{cat}) 1.0 g; F_{sol} = 0.60 mL h^{-1} ($F_{4AOL\text{-}CA}$ = 0.32 mmol h^{-1}); $W_{cat}/F_{4AOL\text{-}CA}$ = 3.2 g h mmol^{-1}; 413 K; 0.9 MPa; TOS 8 h; fixed-bed flow reactor.

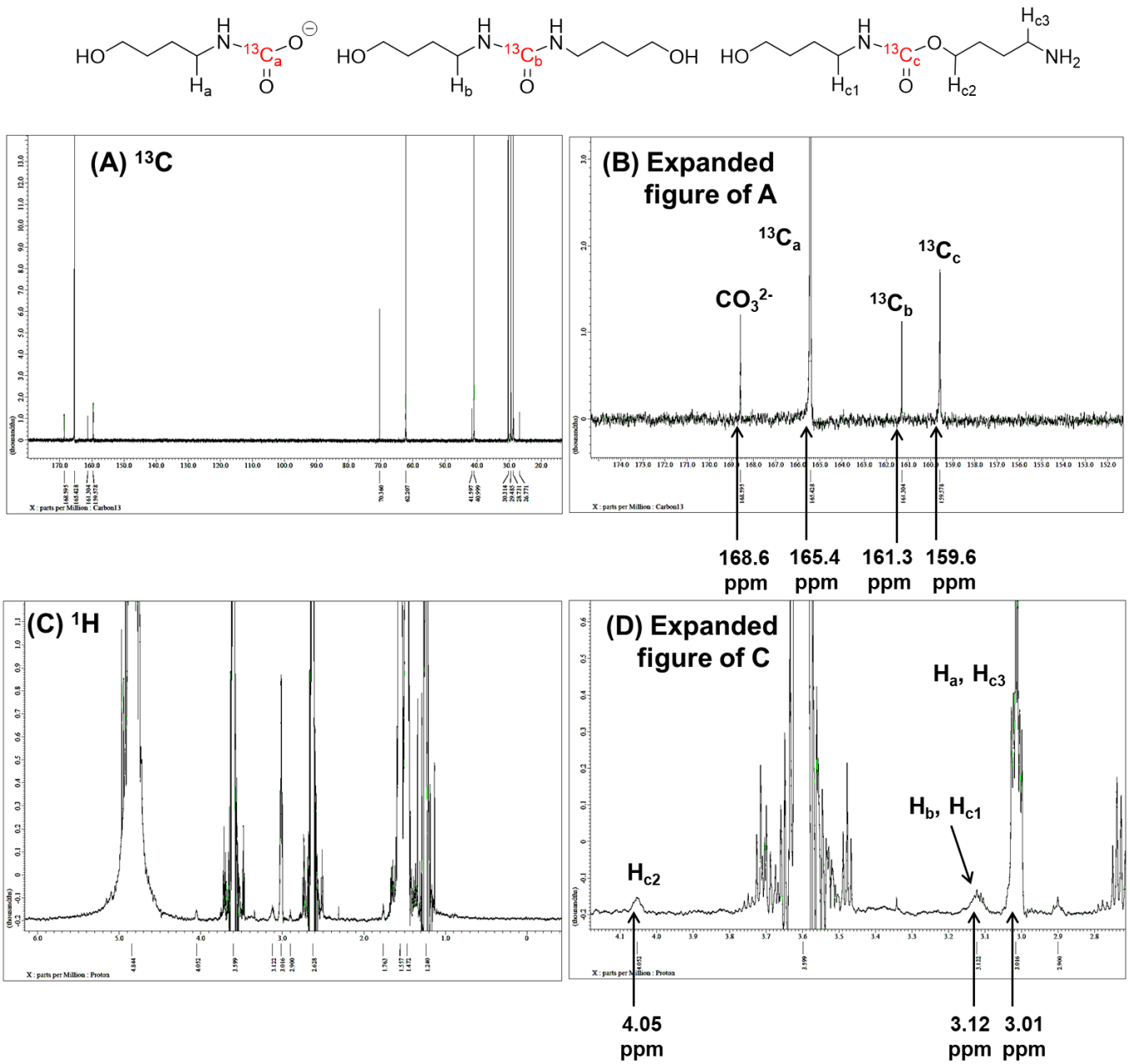

Fig. S17 (A, B) ^{13}C and (C, D) ^{1}H NMR spectra of the reaction mixture after the conversion of 4AOL-CA prepared from ^{13}C-labeled CO_2 in a fixed-bed flow reactor, acquired in D_2O in the presence of *tert*-butyl alcohol as an internal standard. (B) Expanded spectrum of panel A. (D) Expanded spectrum of panel C.
Reaction conditions: 5.0 mol% (= 7.2 wt%) 4AOL-CA in 4AOL solution; CeO_2 with a granule size of 1.0–1.7 mm (W_{cat}) 1.0 g; F_{sol} = 0.60 mL h^{-1} ($F_{4AOL\text{-}CA}$ = 0.25 mmol h^{-1}); $W_{cat}/F_{4AOL\text{-}CA}$ = 3.9 g h $mmol^{-1}$; 393 K; 0.9 MPa; TOS 9 h; fixed-bed flow reactor.

Notes: This ^{13}C NMR spectrum was recorded with the acquisition time that was optimized for quaternary carbon atoms in the C=O moieties (80.8 s for this case; 3.0 s for usual measurements) by measuring longitudinal relaxation time (*i.e.*, T_1). Although ^{13}C-labeled CO_2 was used for preparing 4AOL-CA, the exchange of $^{13}CO_2$-derived moiety in 4AOL-CA with atmospheric $^{12}CO_2$ inevitably proceeded to some extent.

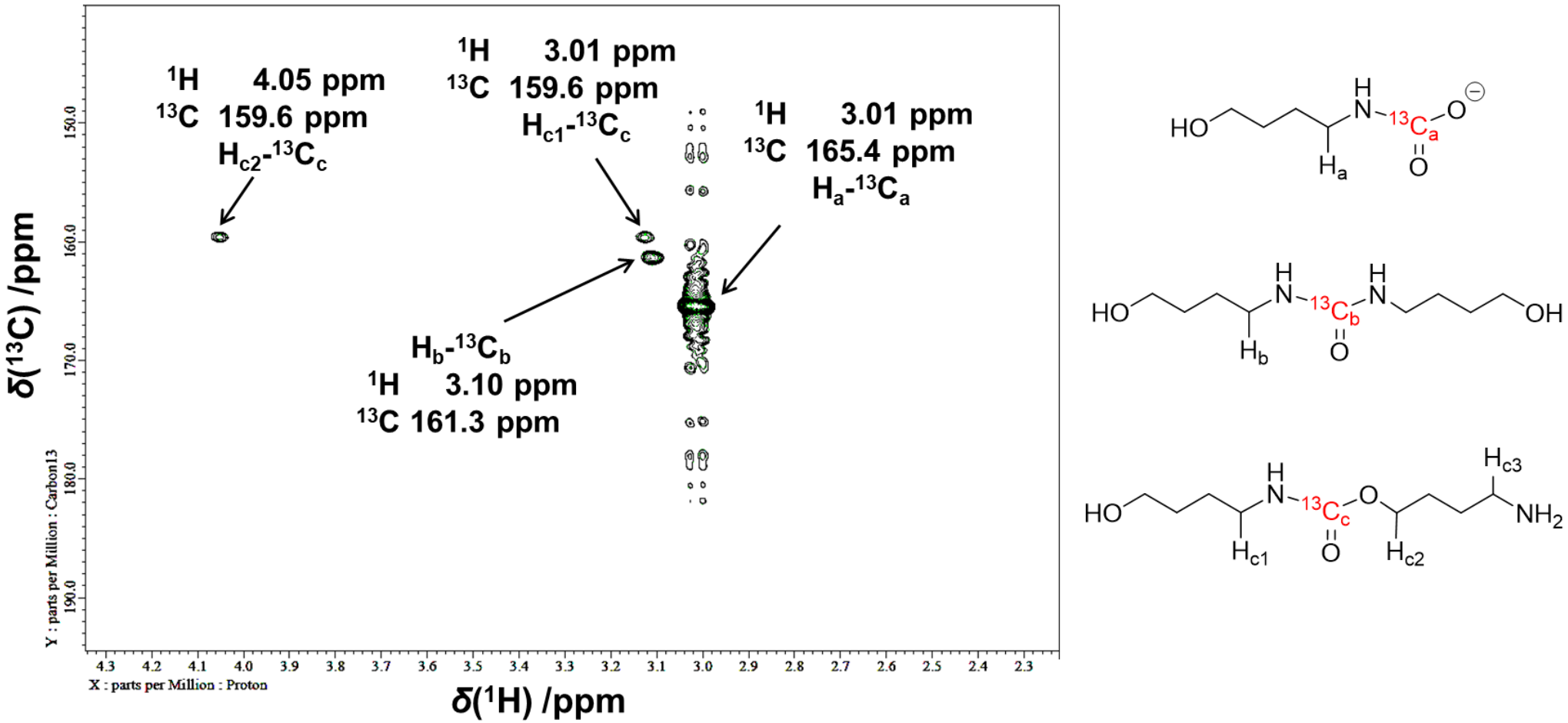

Fig. S18 ^{1}H–^{13}C HMBC spectrum of reaction mixture after the conversion of 4AOL-CA prepared from ^{13}C-labeled CO_2 in 4AOL solvent in a fixed-bed flow reactor, acquired in D_2O. Reaction conditions: 5.0 mol% (= 7.2 wt%) 4AOL-CA in 4AOL solution; CeO_2 with a granule size of 1.0–1.7 mm (W_{cat}) 1.0 g; F_{sol} = 0.60 mL h^{-1} ($F_{4AOL\text{-}CA}$ = 0.25 mmol h^{-1}); $W_{cat}/F_{4AOL\text{-}CA}$ = 3.9 g h $mmol^{-1}$; 393 K; 0.9 MPa; TOS 9 h; fixed-bed flow reactor.

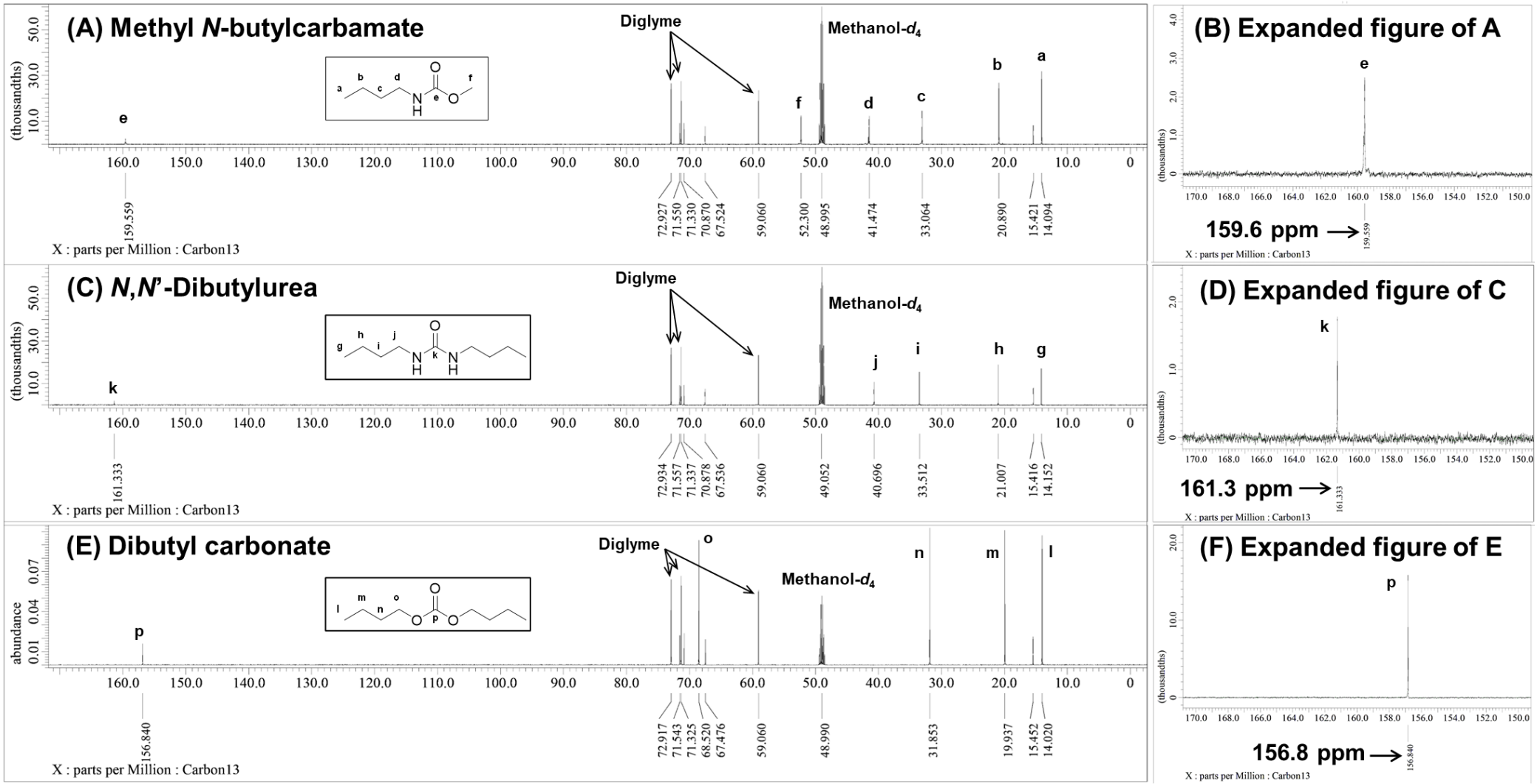

Fig. S19 ^{13}C NMR spectra of various carbonyl compounds purchased from chemical companies, acquired in methanol-d_4 in the presence of diethylene glycol dimethyl ether as an internal standard: (A, B) methyl *N*-butylcarbamate; (C, D) *N*,*N*'-dibutylurea; (E, F) dibutyl carbonate.
The panels B, D, and F are the expanded versions of A, C, and E, respectively.

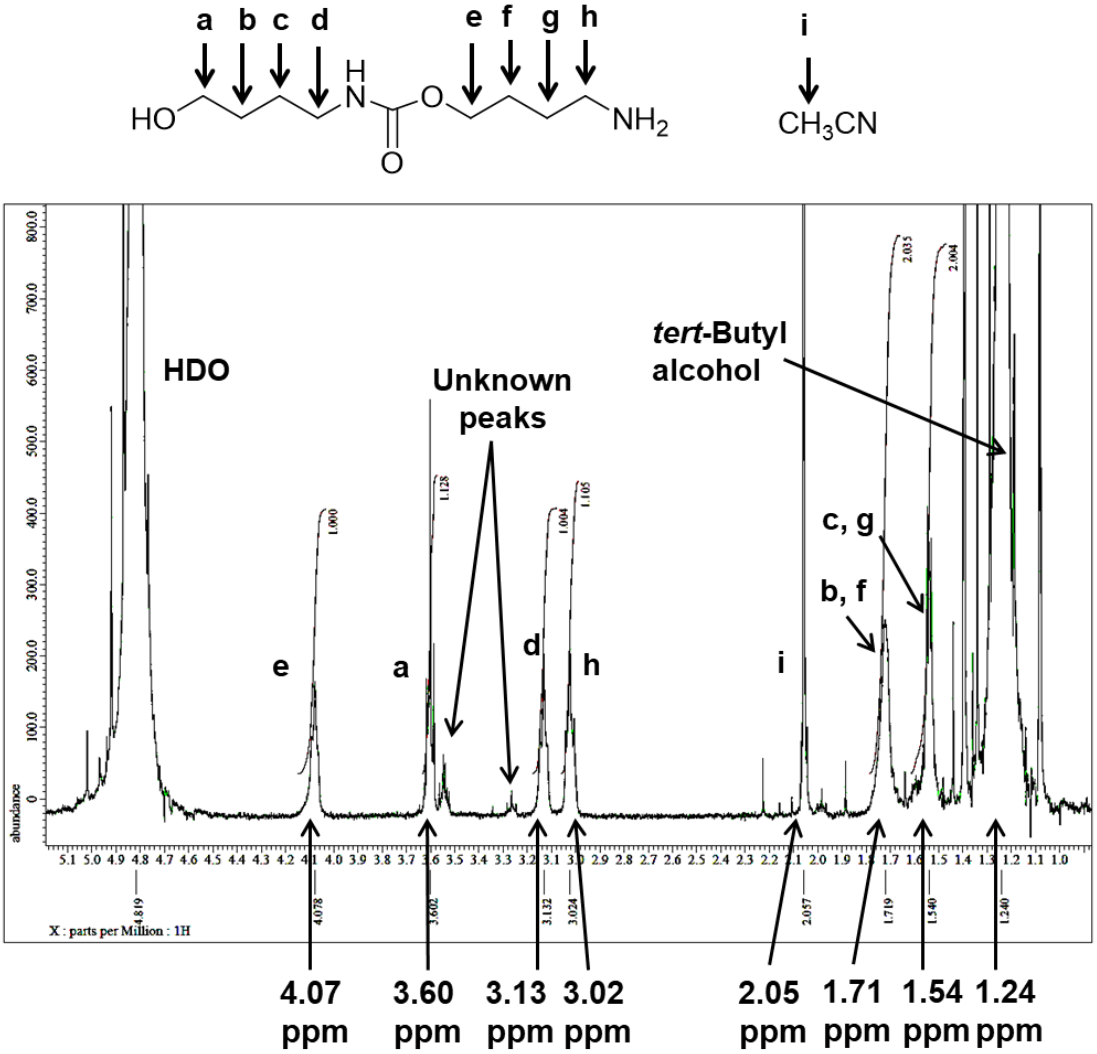

Fig. S20 ^{1}H NMR spectrum of 4LC isolated from the reaction mixture after the conversion of 4AOL-CA in 4AOL solvent over CeO_2 catalyst in a fixed-bed flow reactor, acquired in D_2O in the presence of *tert*-butyl alcohol as an internal standard. Acetonitrile detected in this spectrum (*i.e.*, singlet signal "i") was derived from the mobile phase of HPLC used for the isolation of 4LC from the reaction mixture.
Reaction conditions: 5.0 mol% (= 7.2 wt%) 4AOL-CA in 4AOL solution; CeO_2 with a granule size of 1.0–1.7 mm (W_{cat}) 1.0 g; F_{sol} = 0.60 mL h^{-1} ($F_{4AOL\text{-}CA}$ = 0.25 mmol h^{-1}); $W_{cat}/F_{4AOL\text{-}CA}$ = 3.9 g h mmol^{-1}; 393 K; 0.9 MPa; TOS 9 h; fixed-bed flow reactor.

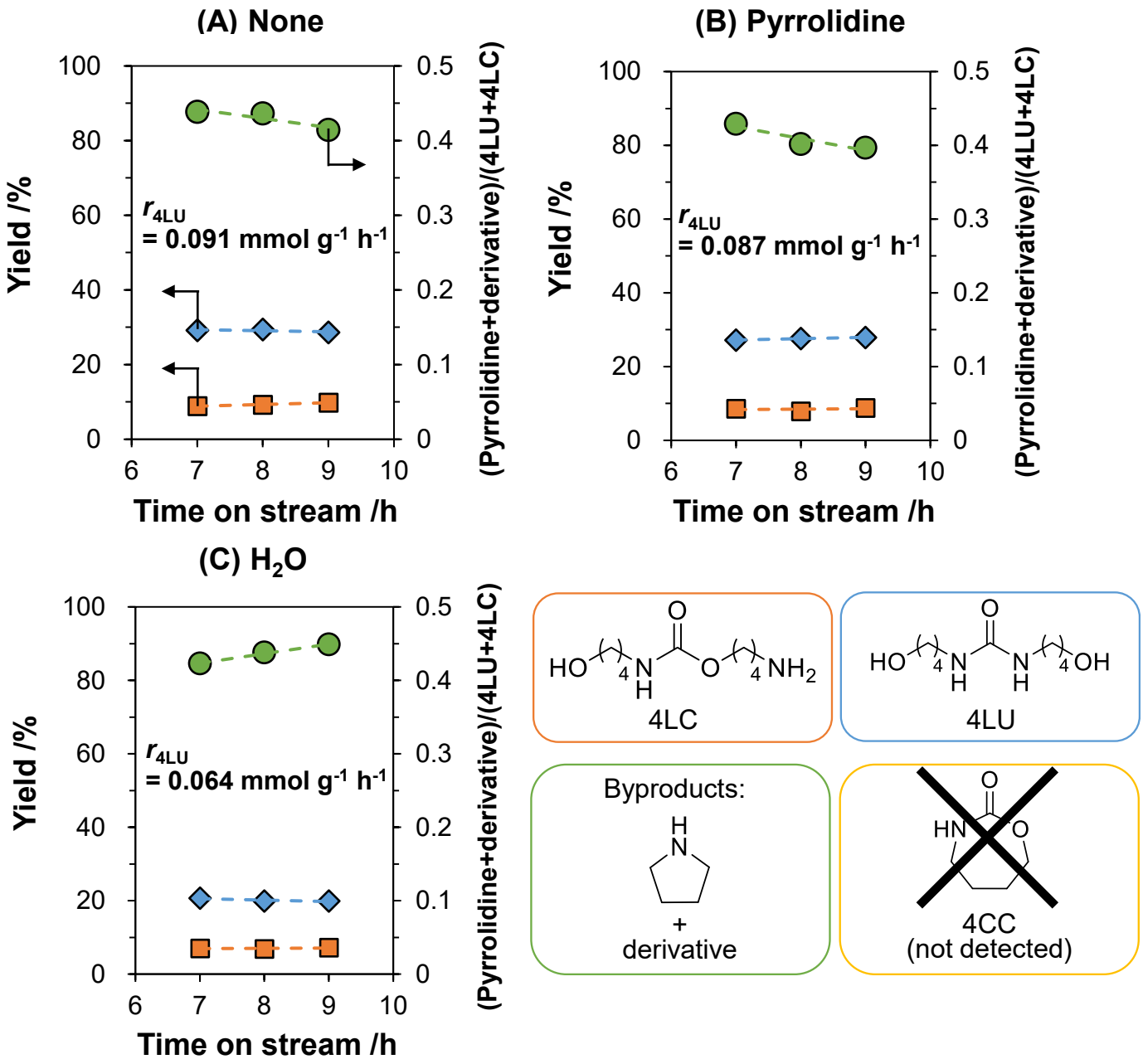

Fig. S21 Effect of additive (either water or pyrrolidine) on the conversion of 4AOL-CA in 4AOL solvent over CeO_2 catalyst at 413 K in a fixed-bed flow-type reactor: (A) without additive; (B) with pyrrolidine; (C) with H_2O.
For panel B, the amount of pyrrolidine was corrected via the subtraction of the amount of pyrrolidine that was intentionally added into the reaction solution.
Reaction conditions: 5.0 mol% (= 7.2 wt%) 4AOL-CA and 0.3 mol% additive (either pyrrolidine or H_2O) in 4AOL solution; CeO_2 with a granule size of 1.0–1.7 mm (W_{cat}) 1.0 g; F_{sol} = 0.60 mL h^{-1} ($F_{4AOL\text{-}CA}$ = 0.32 mmol h^{-1}); $W_{cat}/F_{4AOL\text{-}CA}$ = 3.2 g h $mmol^{-1}$; 413 K; 0.9 MPa; TOS 9 h.
The detailed data are shown in Table S19.

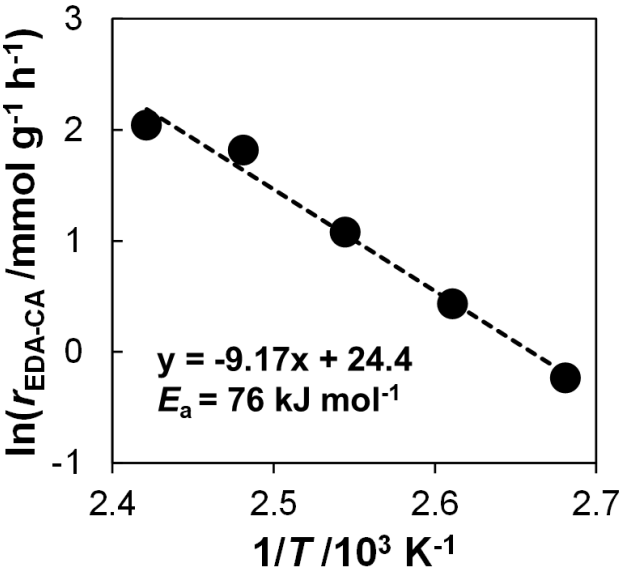

Fig. S22 Arrhenius plot for the conversion of EDA-CA in EDA solvent over CeO_2 catalyst.
Reaction conditions: 5.0 mol% (= 8.4 wt%) EDA-CA in EDA solution; CeO_2 with a granule size of 1.0–1.7 mm (W_{cat}) 0.10–0.15 g; F_{sol} = 2.4–4.8 mL h^{-1} ($F_{EDA\text{-}CA}$ = 1.8–3.7 mmol h^{-1}); $W_{cat}/F_{EDA\text{-}CA}$ = 0.028–0.084 g h $mmol^{-1}$; 373–413 K; 0.9 MPa; TOS 7–9 h; fixed-bed flow reactor.
The detailed data are shown in Table S23.

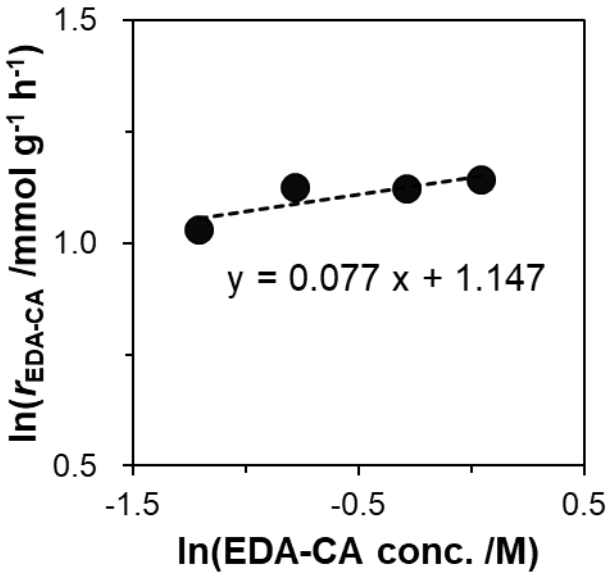

Fig. S23 Double logarithmic plot of the initial conversion rate of EDA-CA as a function of the concentration of EDA-CA in EDA solvent.
Reaction conditions: 2,0–7.0 mol% (= 0.30–1.0 M) EDA-CA in EDA solution; CeO_2 with a granule size of 1.0–1.7 mm (W_{cat}) 0.15 g; F_{sol} = 2.4 mL h^{-1} ($F_{EDA\text{-}CA}$ = 0.72–2.5 mmol h^{-1}); $W_{cat}/F_{EDA\text{-}CA}$ = 0.060–0.21 g h $mmol^{-1}$; 393 K; 0.9 MPa; TOS 9 h; fixed-bed flow reactor.
The detailed data are shown in Table S24.

Temperature /K	413	403	393
r_{DBU} /mmol g^{-1} h^{-1}	0.22	0.076	0.043

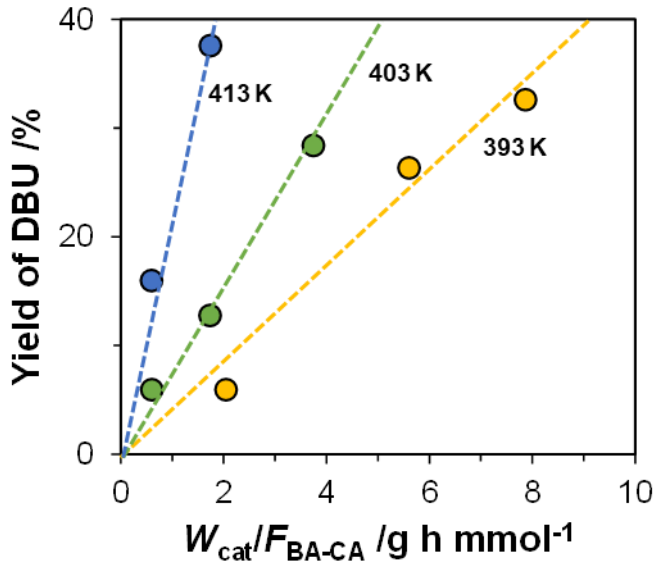

Fig. S24 Initial time courses of BA-CA conversion in BA solvent over CeO_2 catalyst at various temperatures in a fixed-bed flow reactor.
Reaction conditions: 5.0 mol% (= 7.7 wt%) BA-CA in BA solution; CeO_2 with a granule size of 1.0–1.7 mm (W_{cat}) 0.7–2.0 g; F_{sol} = 0.60–2.4 mL h^{-1} (F_{BA-CA} = 0.25–1.2 mmol h^{-1}); W_{cat}/F_{BA-CA} = 0.59–7.9 g h^{-1} mmol^{-1}; 393–413 K; 0.9 MPa; TOS 9–10 h; fixed-bed flow reactor.
The detailed data are shown in Tables S25.

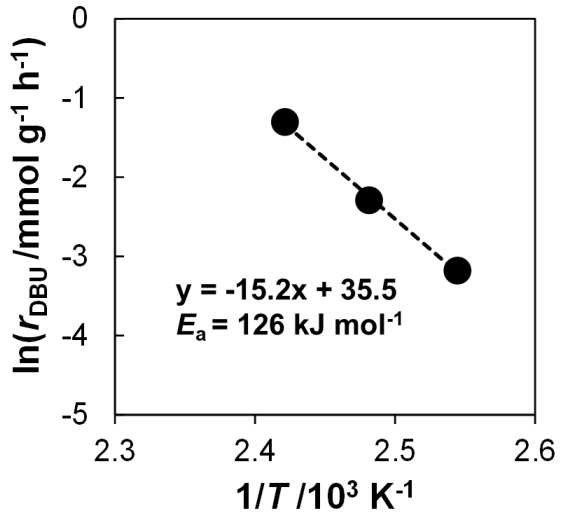

Fig. S25 Arrhenius plot for the conversion of BA-CA in BA solvent over CeO_2 catalyst.
Reaction conditions: 5.0 mol% (= 7.7 wt%) BA-CA in BA solution; CeO_2 with a granule size of 1.0–1.7 mm (W_{cat}) 0.70–2.0 g; F_{sol} = 0.60–2.4 mL h^{-1} (F_{BA-CA} = 0.25–1.2 mmol h^{-1}); W_{cat}/F_{BA-CA} = 0.59–7.9 g h^{-1} mmol^{-1}; 393–413 K; 0.9 MPa; TOS 9–10 h; fixed-bed flow reactor.
The detailed data are shown in Table S26.

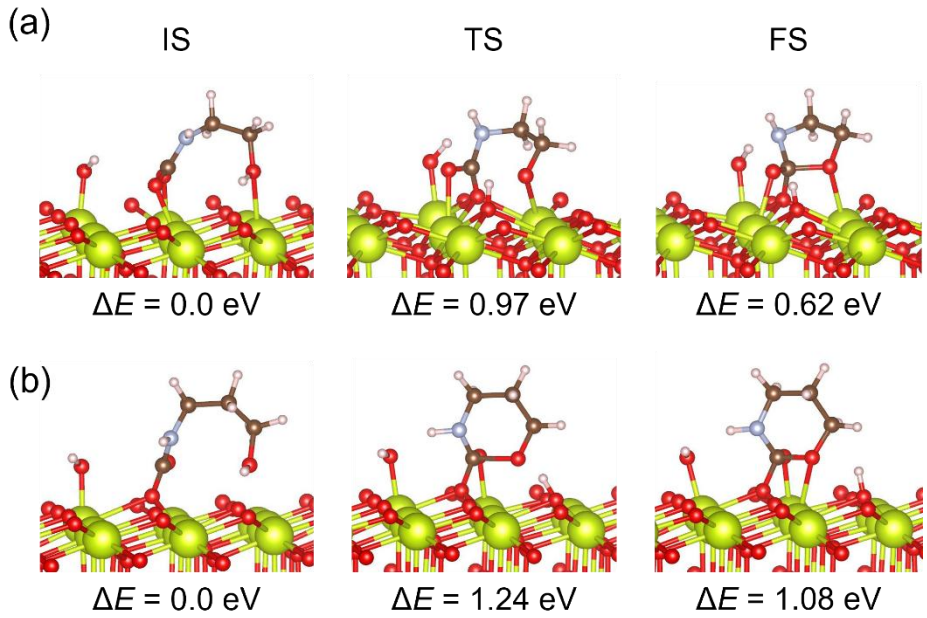

Fig. S26 Structures of the initial state (**IS**), transition state (**TS**), and final state (**FS**) for the cyclization of (a) 2AOL-CA to 2CC and (b) 3AOL-CA to 3CC.
The initial states correspond to the chemisorption structure of a bridged carbamate species and a hydroxy group on the CeO_2 surface, formed via nucleophilic attack of a surface oxygen atom on a carbon atom and concomitant dissociation of the C−O bond. This adsorption structure is analogous to that of EDA-CA species reported in our previous work.[S9]
White, dark brown, red, light blue, and green spheres represent hydrogen, carbon, oxygen, nitrogen, and cerium atoms, respectively.

	Linear carbamates (*Z*-conformation)	Cyclic carbamates (*E*-conformation)
	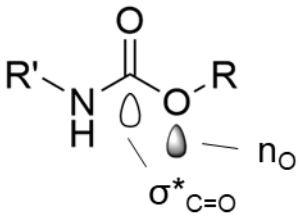	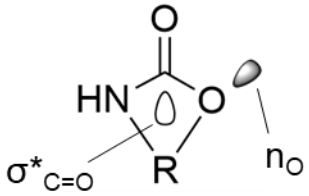
Hyperconjugation ($n_O \rightarrow \sigma^*_{C=O}$)	Presence	Absence
Reactivity	Low	**High**

Fig. S27 Hyperconjugation from lone pair of -OR moiety to unoccupied $\sigma^*_{C=O}$ orbital of C=O structure.

Supplementary references

S1 P. Stringari, G. Scalabrin, A. Valtz and D. Richon, *J. Chem. Thermodyn.*, 2009, **41**, 683–688.

S2 M. A. Casadei, C. Galli and L. Mandolini, *J. Am. Chem. Soc.*, 1984, **106**, 1051–1056.

S3 T. Chen, Z. Qin, Y. Qi, T. Deng, X. Ge, J. Wang and X. Hou, *Polym. Chem.*, 2011, **2**, 1190–1194.

S4 C. Perinu, B. Arstad and K.-J. Jens, *Energy Procedia*, 2013, **37**, 7310–7317.

S5 H. Koizumi, K. Takeuchi, K. Matsumoto, N. Fukaya, K. Sato, M. Uchida, S. Matsumoto, S. Hamura and J.-C. Choi, *Commun. Chem.*, 2021, **4**, 66.

S6 J. Peng, M. Tamura, M. Yabushita, R. Fujii, Y. Nakagawa and K. Tomishige, *ACS Omega*, 2021, **6**, 27527–27535.

S7 D. Su, H. Chen, Q. Yang, H. Liu, M. Lv, Y. Zhao, J. Zhou, Q. Zhang, Z. Lu and L. Chen, *J. CO_2 Util.*, 2024, **83**, 102793.

S8 J. Peng, M. Yabushita, Y. Li, R. Fujii, M. Tamura, Y. Nakagawa and K. Tomishige, *Appl. Catal. A: Gen.*, 2022, **643**, 118747.

S9 R. Fujii, M. Yabushita, D. Asada, M. Tamura, Y. Nakagawa, A. Takahashi, A. Nakayama and K. Tomishige, *ACS Catal.*, 2023, **13**, 1562–1573.

S10 R. Fujii, M. Yabushita, Y. Li, Y. Nakagawa and K. Tomishige, *ACS Catal.*, 2023, **13**, 11041–11056.

S11 S. Mihara, M. Yabushita, Y. Nakagawa and K. Tomishige, *ChemSusChem*, 2024, **18**, e202301436.

S12 H. Koizumi, K. Takeuchi, K. Matsumoto, N. Fukaya, K. Sato, M. Uchida, S. Matsumoto, S. Hamura, J.-C. Choi, One-Pot Synthesis of *N*-Substituted Carbamic Acid Esters from Low Concentrations of CO_2, *ACS Sustainable Chem. Eng.*, 2022, **10**, 5507–5516.

S13 H. Koizumi, K. Takeuchi, K. Matsumoto, N. Fukaya, K. Sato, M. Uchida, S. Matsumoto, S. Hamura, J. Hirota, M. Nakashige and J.-C. Choi, *J. Org. Chem.*, 2023, **88**, 5015–5024.

S14 S. L. Peterson, S. M. Stucka, C. J. Dinsmore, *Org. Lett.*, 2010, **12**, 1340–1343.

S15 H. Matsuda, A. Baba, R. Nomura, M. Kori and S. Ogawa, *Ind. Eng. Chem. Prod. Res. Dev.*, 1985, **24**, 239–242.

S16 S. Fujita, H. Kanamaru, H. Senboku and M. Arai, *Int. J. Mol. Sci.*, 2006, **7**, 438–450.

S17 K. Tominaga and Y. Sasaki, *Synlett*, 2002, 0307–0309.

S18 S. Pulla, C. M. Felton, Y. Gartia, P. Ramidi and A. Ghosh, *ACS Sustainable Chem. Eng.*, 2013, **1**, 309–312.

S19 Y. Takada, S. W. Foo, Y. Yamazaki and S. Saito, *RSC Adv.*, 2014, **4**, 50851–50857.

S20 R. Juárez, P. Concepción, A. Corma and H. García, *Chem. Commun.*, 2010, **46**, 4181–4183.

S21 M. Tamura, M. Honda, K. Noro, Y. Nakagawa and K. Tomishige, *J. Catal.*, 2013, **305**, 191–203.

S22 G. S. More and R. Srivastava, *Ind. Eng. Chem. Res.*, 2021, **60**, 12492–12504.